Calculation of next-to-leading QCD corrections to $b \to sg$

Christoph Greub and Patrick Liniger
Institut für Theoretische Physik, Universität Bern, CH-3012 Bern, Switzerland
(Received 13 September 2000; published 7 February 2001)

In this paper a detailed standard model (SM) calculation of the $O(\alpha_s)$ virtual corrections to the decay width $\Gamma(b \to sg)$ is presented (g denotes a gluon). Also the complete expressions for the corresponding $O(\alpha_s)$ bremsstrahlung corrections to $b \to sg$ are given. The combined result is free of infrared and collinear singularities, in accordance with the KLN theorem. Taking into account the existing next-to-leading logarithmic (NLL) result for the Wilson coefficient $C_8^{\rm eff}$, a complete NLL result for the branching ratio $\mathcal{B}^{\rm NLL}(b \to sg)$ is derived. Numerically, we obtain $\mathcal{B}^{\rm NLL} = (5.0 \pm 1.0) \times 10^{-3}$, which is more than a factor of two larger than the leading logarithmic result $\mathcal{B}^{\rm LL} = (2.2 \pm 0.8) \times 10^{-3}$. The NLL correction is large in spite of the naive suppression factor $\alpha_s(m_b)/\pi$ due to an extra factor of $C_2(m_b)/C_8(m_b) \sim 7$. The impact of these corrections on the inclusive charmless hadronic branching ratio $\overline{\mathcal{B}_\ell}$ of B mesons, which can be used to extract $|V_{ub}/V_{cb}|$ in the context of the SM, is shown to be of similar importance as NLL corrections to b-quark decay modes with three quarks in the final state. Finally, the impact of the NLL corrections to $b \to sg$ on $\overline{\mathcal{B}_\ell}$ is investigated in scenarios, where the Wilson coefficient C_8 is enhanced by new physics.

DOI: 10.1103/PhysRevD.63.054025 PACS number(s): 12.38.Bx, 13.25.Hw

I. INTRODUCTION

The theoretical predictions for inclusive decay rates of B mesons rest on solid grounds due to the fact that these rates can be systematically expanded in powers of $\Lambda_{\rm QCD}/m_b$ [1,2], where the leading term corresponds to the decay width of the underlying b-quark decay. As the power corrections only start at $O(\Lambda_{\rm QCD}^2/m_b^2)$, they affect these rates by at most a few percent. Theoretically, spectator effects of order $16\pi^2(\Lambda_{\rm QCD}/m_b)^3$ [3,4] could be larger [4], but for the decay rates of $B^\pm$ and B^0 they are experimentally known to be at the percent level as well [5]. Thus the accuracy of the theoretical predictions is mainly controlled by our knowledge of the perturbative corrections to the free quark decays.

The inclusive charmless hadronic decays $B \to X_\ell$, where X_ℓ denotes any hadronic charmless final state, are an interesting subclass of the decays mentioned above; as pointed out in Ref. [6], a measurement of the corresponding branching ratio would allow the extraction of the presently poorly known ratio $|V_{ub}/V_{cb}|$, where V_{ub} and V_{cb} are elements of the Cabibbo-Kobayashi-Maskawa (CKM) matrix. At the quark level, there are decay modes with three-body final states, viz. $b \to q' \overline{q'} q$, ($q' = u,d,s; q = d,s$) and the modes $b \to qg$, with two-body final state topology, which contribute to the charmless decay width at leading logarithmic (LL) accuracy. In the very heavy b-quark limit, $b \to qg$ would form one of the dominant contributions to the two-jet decay channel, while $b \to q' \overline{q'} q$ would mainly contribute to 3-jet hadronic final states. However, for the relevant value of the b-quark mass, no jet separation can really be made. Therefore, the decay modes with 2 and 3 partons in the final state have a purely formal, perturbative meaning; physically, they are ''only'' components of the charmless decay rate.

Calculations of next-to-leading logarithmic (NLL) corrections to the three-body decay modes were started already some time ago in Ref. [7], where radiative corrections to the current-current diagrams of the operators O_1 and O_2 were calculated, together with NLL corrections to the Wilson coefficients. Later, Lenz *et al.* included in a first step [8] the contributions of the penguin diagrams associated with the operators O_1 and O_2, and in a second step [6] the same authors also included one-loop penguin diagrams of the penguin operators $O_3, \ldots, O_6$; also the effects of the chromomagnetic operator O_8 were taken into account to the relevant precision needed for a NLL calculation. Up to contributions from current-current type corrections to the penguin operators, the NLL calculation for the three quark final states is now complete.

In the numerical evaluations of the charmless hadronic branching ratio, the two body decay modes $b \to qg$ were added in Refs. [8,6] at the LL precision, as the full NLL predictions were missing. To fill this gap, we recently wrote a short letter where *NLL results* for the branching ratio $\mathcal{B}(b \to sg)$ were presented [9], which includes virtual- and gluon bremsstrahlung corrections to $b \to sg$. In the present work, we describe in detail the non-trivial two-loop *NLL calculation*, which led to the results in [9]. As the NLL corrections enhance $\mathcal{B}(b \to sg)$ by more than a factor of 2, we also analyze in the present paper their impact on the charmless hadronic branching ratio.

At this point, a clarifying remark concerning the terminology should be added: In *experimental* analyses, the term ''$b \to sg$'' usually stands for all the electroweak penguin contributions to the inclusive charmless B meson decay, which in the present paper will be denoted as ''$B \to$ no charm.'' In our work, $b \to sg$ denotes a b-quark decaying into an s-quark and an on-shell gluon, which is just one particular contribution to $B \to$ no charm, as discussed above.

The decay $b \to sg$ gained a lot of attention in the last years. For a long time the theoretical predictions for both, the inclusive semileptonic branching ratio $\mathcal{B}_{\rm sl}$ and the charm multiplicity n_c in B-meson decays were considerably higher than the experimental values [10]. An attractive hypothesis, which would move the theoretical predictions for both ob-

servables into the direction favored by the experiments, assumed the rare decay mode $b \to sg$ to be enhanced by new physics.

After the inclusion of the complete NLL corrections to the decay modes $b \to c\bar{u}q$ and $b \to c\bar{c}q (q=d,s)$ [11], the theoretical prediction for the semileptonic branching ratio and the charm multiplicity [4] are

$$\mathcal{B}_{\rm sl}^{\rm th} = (11.7 \pm 1.4 \pm 1.0)\%, \quad n_c^{\rm th} = 1.20 \pm 0.06, \tag{1}$$

where the second error in $\mathcal{B}_{\rm sl}^{\rm th}$ takes into account the spectator effects estimated in Ref. [4]. The experimental results from measurements at the $\Upsilon(4S)$ resonance and those from the Z^0 resonance at the CERN e^+e^- collider LEP and SLAC Large Detector (SLD) were recently summarized [12] to be

$$\mathcal{B}_{\rm sl}^{\Upsilon(4S)} = (10.45 \pm 0.21)\%, \quad n_c^{\Upsilon(4S)} = 1.14 \pm 0.06,$$

$$\mathcal{B}_{\rm sl}^{Z^0} = (10.79 \pm 0.25)\%, \quad n_c^{Z^0} = 1.17 \pm 0.04. \tag{2}$$

We would like to stress that in the theoretical results the renormalization scale was taken in the interval $[m_b/4, 2m_b]$. If one only considers $\mu \in [m_b/2, 2m_b]$, the theoretical predictions would only have marginal overlap with experimental data. This implies that there is still room for enhanced $b \to sg$. We therefore also illustrate in this paper the influence of the NLL corrections to $b \to sg$ on the charmless hadronic branching ratio in scenarios where the Wilson coefficient C_8 is enhanced by new physics.

We also would like to mention that the component $b \to sg$ of the charmless hadronic decays is expected to manifest itself in kaons with high momenta (of order $m_b/2$), due to its two body nature [13]. Some indications for enhanced $b \to sg$ in this context were reported by the SLD Collaboration [14]. For a review of other hints for enhanced $b \to sg$, the reader is referred to [15].

Within the SM, the LL prediction for the branching for $b \to sg$ is known to be $\mathcal{B}(b \to sg) \approx 0.2\%$ [16]. The process $b \to sgg$, which gives a NLL contribution to the inclusive charmless decay width has already been studied in the literature [17,18]. In [18] a complete calculation was performed in regions of the phase space which are free of collinear an infrared singularities. Putting suitable cuts, the branching ratio for $b \to sgg$ was found to be of the order 10^{-3} in these phase space regions. A complete calculation requires the calculation of a regularized version for the decay width $\Gamma(b \to sgg)$ in which infrared and collinear singularities become manifest. Only after adding the virtually corrected decay width $\Gamma(b \to sg)$ a finite result is obtained.

We anticipate, that we find large NLL corrections to the decay rate $\Gamma(b \to sg)$. For the corresponding branching ratio we obtain $\mathcal{B}^{\rm NLL} = (5.0 \pm 1.0) \times 10^{-3}$, which is more than a factor of two larger than the leading logarithmic result $\mathcal{B}^{\rm LL} = (2.2 \pm 0.8) \times 10^{-3}$. The reason for the large NLL correction can be explained as follows: At leading logarithmic precision, the decay amplitude $A(b \to sg)$ is given by the tree-level matrix element of $C_8(m_b)O_8(m_b)$ alone; due to reasons of gauge invariance, there is no one-loop contribution of $C_2(m_b)O_2(m_b)$. The LL branching ratio is therefore proportional to the square of the rather small Wilson coefficient $|C_8(m_b)| \sim 0.15$. At NLL order, $C_2(m_b)O_2(m_b)$ does contribute to the decay amplitude $A(b \to sg)$, leading to a term $\sim (\alpha_s/\pi) C_2(m_b) C_8(m_b)$ at the level of the branching ratio. The naive suppression factor $\alpha_s(m_b)/\pi$ is enhanced by an extra factor $|C_2(m_b)/C_8(m_b)| \sim 7$; this explains the unusually large NLL correction. A more detailed discussion in Sec. IX indicates that next order corrections should be under control; in particular, the large NLL corrections do not signal the breakdown of renormalization group improved perturbation theory.

The remainder of this paper is organized as follows: In Sec. II, we review the theoretical framework and discuss the steps needed for a NLL calculation for $\mathcal{B}(b \to sg)$. Section III is devoted to the calculation of the virtual corrections to the matrix elements $\langle sg|O_{1,2}|b\rangle$, including renormalization, while Sec. IV deals with virtual corrections to $\langle sg|O_8|b\rangle$. In Sec. V the virtual corrections to the decay width $\Gamma(b \to sg)$ are calculated. Sections VI and VII deal with the gluon bremsstrahlung matrix elements $\langle sgg|O_{1,2,8}|b\rangle$ and the corresponding decay width, respectively. The analytic results for the NLL branching ratio $\mathcal{B}(b \to sg)$ can be found in Sec. VIII, while the numerical evaluations are presented in Sec. IX. Section X deals with the impact of the NLL corrections to $\mathcal{B}(b \to sg)$ on the charmless hadronic branching ratio in the standard model, while in Sec. XI similar questions are addressed in scenarios where the Wilson coefficient C_8 is enhanced by new physics. We conclude with a short summary in Sec. XII. An explicit parametrization of the NLL Wilson coefficient $C_8^{\rm eff}(m_b)$ is given in Appendix A.

II. THE EFFECTIVE HAMILTONIAN

We use the framework of an effective low-energy theory with five quarks, obtained by integrating out the heavy degrees of freedom, which in the SM are the *t*-quark and the *W*-boson. We take into account operators up to dimension six and we put $m_s = 0$. In this approximation the effective Hamiltonian relevant for radiative decays and $b \to sg(g)$ reads

$$\mathcal{H}_{\rm eff} = -\frac{4G_F}{\sqrt{2}} V_{ts}^* V_{tb} \sum_{i=1}^{8} C_i(\mu) O_i(\mu), \tag{3}$$

where G_F is the Fermi coupling constant and $C_i(\mu)$ are the Wilson coefficients evaluated at the scale μ; V_{tb} and V_{ts} are matrix elements of the Cabibbo-Kobayashi-Maskawa (CKM) matrix. The operators O_i read [19]

$$O_1=(\bar{s}_L\gamma_\mu T^A c_L)(\bar{c}_L\gamma^\mu T^A b_L), \qquad O_2=(\bar{s}_L\gamma_\mu c_L)(\bar{c}_L\gamma^\mu b_L),$$

$$O_3=(\bar{s}_L\gamma_\mu b_L)\sum_q (\bar{q}\gamma^\mu q), \qquad O_4=(\bar{s}_L\gamma_\mu T^A b_L)\sum_q (\bar{q}\gamma^\mu T^A q),$$

$$O_5=(\bar{s}_L\gamma_\mu\gamma_\nu\gamma_\rho b_L)\sum_q (\bar{q}\gamma^\mu\gamma^\nu\gamma^\rho q), \qquad O_6=(\bar{s}_L\gamma_\mu\gamma_\nu\gamma_\rho T^A b_L)\sum_q (\bar{q}\gamma^\mu\gamma^\nu\gamma^\rho T^A q),$$

$$O_7=\frac{e}{16\pi^2}\bar{m}_b(\mu)(\bar{s}_L\sigma^{\mu\nu}b_R)F_{\mu\nu}, \qquad O_8=\frac{g_s}{16\pi^2}\bar{m}_b(\mu)(\bar{s}_L\sigma^{\mu\nu}T^A b_R)G^A_{\mu\nu}. \tag{4}$$

In the dipole operators O_7 (O_8), e and $F_{\mu\nu}$ (g_s and $G^A_{\mu\nu}$) denote the electromagnetic (strong) coupling constant and field strength tensor, respectively. $T^A(A=1,\ldots,8)$ are $SU(3)$ color generators; $L=(1-\gamma_5)/2$ and $R=(1+\gamma_5)/2$ stand for left- and right-handed projectors. The index q in the sum Σ_q runs over all quarks except the t-quark. In Eq. (4), $\bar{m}_b(\mu)$ is the running b-quark mass in the modified minimal subtraction ($\overline{\rm MS}$) scheme at the renormalization scale μ. Henceforth, $\bar{m}_q(\mu)$ and m_q denote $\overline{\rm MS}$ running and pole masses, respectively. To first order in α_s, these masses are related through

$$\bar{m}_q(\mu)=m_q\left(1+\frac{\alpha_s(\mu)}{\pi}\ln\frac{m_q^2}{\mu^2}-\frac{4}{3}\frac{\alpha_s(\mu)}{\pi}\right). \tag{5}$$

It is well known that QCD corrections to the decay rate for $b\to s\gamma$ bring in logarithms of the mass ratios m_b/m_W and m_b/m_t. The same is true for the process $b\to sg$: QCD corrections to this process induce terms of the form $\alpha_s\alpha_s^n\ln^m(m_b/M)$, where $M=m_t$ or m_W and $m\leqslant n$ (with $m,n=0,1,2,\ldots$).

One can systematically resum these large terms by renormalization group techniques. Usually, one matches the full standard model theory with the effective theory at a scale of order m_W. At this scale, the large logarithms generated by matrix elements in the effective theory are the same ones as in the full theory. Consequently, the Wilson coefficients only pick up formally small QCD corrections. Using the renormalization group equation, the Wilson coefficients are then calculated at the scale $\mu=\mu_b\approx m_b$, at which the large logarithms are contained in the Wilson coefficients, while the matrix elements of the operators are free of them.

So far the decay rate for $b\to sg$ has been systematically calculated only to leading logarithmic (LL) accuracy, i.e., for $m=n$.

A consistent calculation for $b\to sg$ at LL precision requires the following steps:

(1) the extraction of the Wilson coefficients from a matching calculation of the full standard model theory with the effective theory at the scale $\mu=\mu_W$ to order α_s^0; μ_W denotes a scale of order m_W or m_t;

(2) a renormalization group treatment of the Wilson coefficients, using the anomalous-dimension matrix to order α_s^1;

(3) the calculation of the decay matrix elements $\langle sg|C_iO_i|b\rangle$ at the scale $\mu=\mu_b$ to order g_s; μ_b denotes a scale of order m_b. We note that the matrix elements associated with the four Fermi operators ($i=1-6$) can be absorbed into the effective Wilson coefficient $C_8^{\rm eff}$, when working at LL precision. In the naive dimensional regularization scheme (NDR), which we use in this paper, one obtains [19]

$$C_8^{\rm eff}=C_8+C_3-\tfrac{1}{6}C_4+20C_5-\tfrac{10}{3}C_6. \tag{6}$$

From the analogous decay $b\to s\gamma$ it is well-known that next-to-leading logarithmic (NLL) corrections drastically reduce the large renormalization scale dependence of the LL branching ratio. This implies, in particular, that the NLL corrections are relatively large, at least for certain scales (within the usually considered range $m_b/2\leqslant\mu_b\leqslant 2m_b$). Motivated by the situation in this analogous process, we present in this paper a systematic calculation of the NLL corrections to $b\to sg$.

TABLE I. Wilson coefficients $C_i^0(\mu)(i=1,\ldots,8)$, $C_8^{1,\rm eff}$, and $C_8^{\rm eff}$ [see Eq. (7) in the text] at the matching scale $\mu=m_W=80.33$ GeV and at three other scales, $\mu=9.6$ GeV, $\mu=4.8$ GeV and $\mu=2.4$ GeV. For $\alpha_s(\mu)$ (in the $\overline{\rm MS}$ scheme) we used the two-loop expression with 5 flavors and $\alpha_s(m_Z)=0.119$. The entries correspond to the pole top quark mass $m_t=175$ GeV.

	$\mu=m_W$	$\mu=9.6$ GeV	$\mu=4.8$ GeV	$\mu=2.4$ GeV
α_s	0.121	0.182	0.218	0.271
C_1^0	0.0	−0.335	−0.497	−0.711
C_2^0	1.0	1.012	1.025	1.048
C_3^0	0.0	−0.002	−0.005	−0.010
C_4^0	0.0	−0.042	−0.067	−0.103
C_5^0	0.0	0.0002	0.0005	0.001
C_6^0	0.0	0.0005	0.001	0.002
C_7^0	−0.192	−0.285	−0.324	−0.371
C_8^0	−0.096	−0.136	−0.150	−0.166
$C_7^{0,\rm eff}$	−0.196	−0.280	−0.314	−0.356
$C_8^{0,\rm eff}$	−0.097	−0.135	−0.149	−0.165
$C_8^{1,\rm eff}$	−2.166	−1.318	−1.098	−0.950
$C_8^{\rm eff}$	−0.118	−0.154	−0.168	−0.186

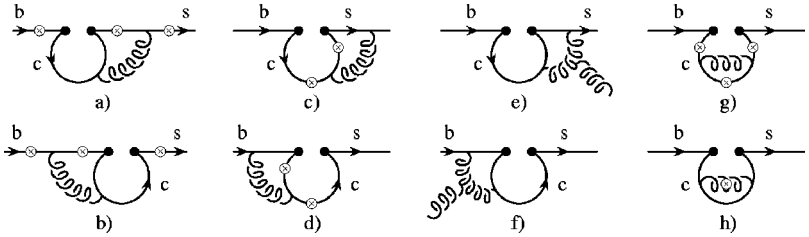

FIG. 1. Graphs associated with the operators $\hat{O}_1$ and $\hat{O}_2$. The wavy lines represent gluons; the real gluons are understood to be attached to the circle-crosses.

The principal organization of such a calculation is straightforward: Each of the three steps listed above has to be improved by going to the next order in α_s: (1) The matching has to be calculated including α_s corrections; (2) the renormalization group treatment of the Wilson coefficients has to be performed using the anomalous dimension matrix to order α_s^2; (3) finally, the order α_s corrections to the decay matrix elements have to be worked out. We note that this step involves both, the calculation of *virtual*- and *bremsstrahlung* corrections to $b \to sg$.

The first two steps are already available in the literature. The order α_s matching of the dipole operators O_7 and O_8 was calculated in Refs. [20], while the matching conditions and the anomalous dimension matrix for the four Fermi operators have been calculated by several groups [21]. These calculations were done in the ''old operator basis,'' introduced by Grinstein *et al.* [22]. The most difficult part, the order α_s^2 mixing of the four-Fermi operators into the dipole operators requires the calculation of three loop diagrams [19]. In order to perform a consistent naive dimensional regularization (NDR) calculation (i.e., with anticommuting γ_5), the old operator basis was replaced by the new one displayed in Eq. (4). The full 8×8 anomalous dimension matrix, the corresponding matching conditions and the definition of the evanescent operators is given in Ref. [19] and is repeated in Appendix A of the present paper.

Step (3), the calculation of the virtual $O(\alpha_s)$ corrections to the matrix elements $M_i = \langle sg|O_i|b\rangle$, as well as the evaluation of the gluon bremsstrahlung process $b \to sgg$, is performed the first time in the present paper. As illustrated in Table I, the LL Wilson coefficients $C_3^0(\mu_b), \ldots, C_6^0(\mu_b)$ are much smaller than $C_1^0(\mu_b)$ and $C_2^0(\mu_b)$. We therefore only calculate M_1, M_2, and M_8 together with the corresponding bremsstrahlung corrections. As M_1 and M_2 vanish at one-loop (i.e., without QCD corrections), only the leading order pieces, $C_1^0(\mu_b)$ and $C_2^0(\mu_b)$, appearing in the decomposition

$$C_i(\mu_b) = C_i^0(\mu_b) + \frac{\alpha_s(\mu_b)}{4\pi} C_i^1(\mu_b) \tag{7}$$

of the NLL Wilson coefficients $C_1(\mu_b)$ and $C_2(\mu_b)$ are needed. On the other hand, the operator O_8 contributes to M_8 already at tree level. Consequently the full NLL Wilson coefficient $C_8^{\rm eff}(\mu_b)$ is needed. The numerical value of the NLL piece $C_8^{1,\rm eff}$ [defined as in Eqs. (6) and (7)] is also given in Table I, while the analytic form is relegated to Appendix A.

III. VIRTUAL CORRECTIONS TO O_1 AND O_2

In this section we present the calculation of the matrix elements of the operator O_1 and O_2 for $b \to sg$ up to order α_s in the NDR scheme. The one-loop (α_s^0) matrix elements vanish and we must consider several two-loop contributions. Since they involve ultraviolet singularities also counterterm contributions are needed. These are easy to obtain, because the operator renormalization constants Z_{ij} are known with enough accuracy from the order α_s anomalous dimension matrix [19].

A. Regularized two-loop matrix elements of O_1 and O_2

For the following discussion it is useful to define the operators $\hat{O}_1$ and $\hat{O}_2$:

$$\hat{O}_1 = 2O_1 + \tfrac{1}{3}O_2; \quad \hat{O}_2 = O_2. \tag{8}$$

$\hat{O}_1$ and $\hat{O}_2$ are nothing but the current-current operators in the old basis [22]:

$$\hat{O}_1 = (\bar{s}_{L\alpha}\gamma_\mu c_{L\beta})(\bar{c}_{L\beta}\gamma^\mu b_{L\alpha}),$$
$$\hat{O}_2 = (\bar{s}_{L\beta}\gamma_\mu c_{L\beta})(\bar{c}_{L\alpha}\gamma^\mu b_{L\alpha}). \tag{9}$$

We now present the calculation of the matrix elements $\hat{M}_i = \langle sg|\hat{O}_i|b\rangle$: The dimensionally regularized matrix element $\hat{M}_2$ is obtained by calculating the two-loop diagrams (a)–(h) shown in Fig. 1.

We start with the calculation of the diagrams (a)–(f) in Fig. 1, in which the virtual gluon connects the charm quark in the loop with an external fermion leg.[1] The main steps of the calculation are the following: We first calculate the Fermion loops in the individual diagrams, i.e., the ''building blocks'' I_β and $J_{\alpha\beta}$ shown in Fig. 2; $J_{\alpha\beta}$ denotes the sum of the the two diagrams on the right.

We work in $d = 4 - 2\epsilon$ dimensions; the results of the building blocks are presented as integrals over Feynman parameters after integrating over the (shifted) loop-momentum. Then we insert these building blocks into the full two-loop diagrams. Using one more Feynman parametrization, we calculate the integral over the second loop-momentum. As the remaining Feynman parameter integrals contain rather complicated denominators, we do not evaluate them directly. At

[1]The diagrams (g) and (h) are much easier to calculate than those in (a)–(f), because m_c is the only scale in the corresponding integrals.

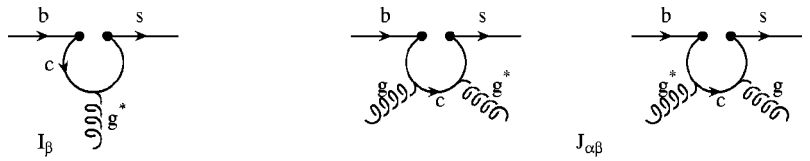

FIG. 2. Building block I_β (with an off-shell gluon) for the diagrams (a), (b), (e), and (f) in Fig. 1 and building block $J_{\alpha\beta}$ for the diagrams (c) and (d) in Fig. 1. $g*$ and g denote an off-shell and an on-shell gluon, respectively.

this level we also do not expand in the regulator ϵ. The heart of our procedure which will be explained more explicitly below, is to represent these denominators as complex Mellin-Barnes integrals [23]. After inserting this representation and interchanging the order of integration, the Feynman parameter integrals are reduced to well-known Euler beta functions. Finally, the residue theorem allows to write the result of the remaining complex integral as the sum over the residues taken at the pole positions of beta and gamma functions; this naturally leads to an expansion in the ratio $z=(m_c/m_b)^2$, which numerically is about $z=0.1$.

We express the diagram on the left in Fig. 2 (denoted by I_β) in a way convenient for inserting into the two-loop diagrams. As we will use $\overline{\text{MS}}$ subtraction later on, we introduce the renormalization scale in the form $\mu^2\underline{\exp(\gamma_E)}/(4\pi)$, where $\gamma_E\approx 0.577$ is the Euler constant. Then, $\overline{\text{MS}}$ corresponds to subtracting the poles in ϵ. In the NDR scheme, I_β is given by[2]

$$I_\beta^A = -\frac{g_s}{4\pi^2}\Gamma(\epsilon)\mu^{2\epsilon}\exp(\gamma_E\epsilon)(1-\epsilon) \times\exp(i\pi\epsilon)T^A(r_\beta \not{r} - r^2\gamma_\beta)L\int_0^1[x(1-x)]^{1-\epsilon} \times\left[r^2-\frac{m_c^2}{x(1-x)}+i\delta\right]^{-\epsilon}, \tag{10}$$

where r is the four-momentum of the (off-shell) gluon, m_c is the mass of the charm quark propagating in the loop and the term $i\delta$ is the ''ϵ-prescription.'' The free index β will be contracted with the gluon propagator when inserting the building block into the two-loop diagrams (a), (b), (e), and (f) in Fig. 1. Note that I_β is gauge invariant in the sense that $r^\beta I_\beta = 0$.

Next we give the sum of the two diagrams on the right in Fig. 2, using the decomposition in [18]. The on-shell gluon has momentum q, color A and polarization α (therefore we drop the terms q^2 and q_α), while the off-shell gluon has momentum r, color B and polarization β. This building block, denoted by $J_{\alpha\beta}^{AB}$, can be decomposed with respect to the color structure as

$$J_{\alpha\beta}^{AB} = T_{\alpha\beta}^+(q,r)\{T^A,T^B\} + T_{\alpha\beta}^-(q,r)[T^A,T^B]. \tag{11}$$

The quantities $T_{\alpha\beta}^+(q,r)$ and $T_{\alpha\beta}^-(q,r)$ read

$$T_{\alpha\beta}^+(q,r) = \frac{g_s^2}{32\pi^2}\Big[E(\alpha,\beta,r)\Delta i_5 + E(\alpha,\beta,q)\Delta i_6 - E(\beta,r,q)\frac{r_\alpha}{(qr)}\Delta i_{23} - E(\alpha,r,q)\frac{r_\beta}{(qr)}\Delta i_{25} - E(\alpha,r,q)\frac{q_\beta}{(qr)}\Delta i_{26}\Big]L, \tag{12}$$

$$T_{\alpha\beta}^-(q,r) = \frac{g_s^2}{32\pi^2}\Big[\not{r} g_{\alpha\beta}\Delta i_2 + \not{q} g_{\alpha\beta}\Delta i_3 + \gamma_\beta r_\alpha \Delta i_8 + \gamma_\alpha r_\beta \Delta i_{11} + \gamma_\alpha q_\beta \Delta i_{12} + \not{r}\frac{r_\alpha r_\beta}{(qr)}\Delta i_{15} + \not{r}\frac{r_\alpha q_\beta}{(qr)}\Delta i_{17} + \not{q}\frac{r_\alpha r_\beta}{(qr)}\Delta i_{19} + \not{q}\frac{r_\alpha q_\beta}{(qr)}\Delta i_{21}\Big]L. \tag{13}$$

The matrix E in Eq. (12) is defined as

$$E(\alpha,\beta,r) = \gamma_\alpha\gamma_\beta\not{r} - \gamma_\alpha r_\beta + \gamma_\beta(r_\alpha) - \not{r} g_{\alpha\beta}. \tag{14}$$

In a four-dimensional context these E quantities can be reduced to expressions involving the Levi-Cività tensor, i.e., $E(\alpha,\beta,\gamma) = -i\varepsilon_{\alpha\beta\gamma\mu}\gamma^\mu\gamma_5$ (in the Bjorken-Drell convention). The dimensionally regularized expressions for the Δi functions read

$$\Delta i_5 = -4B^+\int_S dxdyC^{-1-\epsilon}[4(qr)x^2y\epsilon - 4(qr)xy\epsilon - 2r^2x^3\epsilon + 3r^2x^2\epsilon - r^2x\epsilon + 3xC - C] \tag{15}$$

$$\Delta i_6 = 4B^+\int_S dxdyC^{-1-\epsilon}[4(qr)xy^2\epsilon - 4(qr)xy\epsilon - 2r^2x^2y\epsilon + 2r^2x^2\epsilon + r^2xy\epsilon - 2r^2x\epsilon + 3yC - C] \tag{16}$$

$$\Delta i_{23} = -\Delta i_{26} = 8B^+(qr)\epsilon\int_S dxdyC^{-1-\epsilon}xy \tag{17}$$

$$\Delta i_{25} = -8B^+(qr)\epsilon\int_S dxdyC^{-1-\epsilon}x(1-x) \tag{18}$$

[2]The fermion/gluon and the fermion/photon couplings are defined according to the covariant derivative $D=\partial+ig_sT^BA^B+ieQA$ where $T^B=\lambda^B/2$ are the SU(3) generators.

$$\Delta i_2 = 4B^- \int_S dxdy C^{-1-\epsilon}(1-x)[4(qr)xy\epsilon - 2r^2x^2\epsilon + r^2x\epsilon + C] \tag{19}$$

$$\Delta i_3 = 4B^- \int_S dxdy C^{-1-\epsilon}[4(qr)xy^2\epsilon - 4(qr)xy\epsilon - 2r^2x^2y\epsilon + 2r^2x^2\epsilon + r^2xy\epsilon - 2r^2x\epsilon + yC - C] \tag{20}$$

$$\Delta i_8 = -4B^- \int_S dxdy C^{-1-\epsilon}[4(qr)x^2y\epsilon + 2(qr)xy\epsilon - 2r^2x^3\epsilon + r^2x^2\epsilon + r^2x\epsilon + xC + C] \tag{21}$$

$$\Delta i_{11} = 4B^- \int_S dxdy C^{-1-\epsilon}(1-x)[4(qr)xy\epsilon - 2(qr)x\epsilon - 2r^2x^2\epsilon + r^2x\epsilon + C] \tag{22}$$

$$\Delta i_{12} = 4B^- \int_S dxdy C^{-1-\epsilon}[4(qr)xy^2\epsilon + 2(qr)xy\epsilon - 2r^2x^2y\epsilon - 2r^2x^2\epsilon + r^2xy\epsilon + 2r^2x\epsilon + yC + C] \tag{23}$$

$$\Delta i_{15} = 16B^-(qr)\epsilon \int_S dxdy C^{-1-\epsilon}x^2(1-x) \tag{24}$$

$$\Delta i_{17} = -8B^-(qr)\epsilon \int_S dxdy C^{-1-\epsilon}xy(1-2x) \tag{25}$$

$$\Delta i_{19} = 8B^-(qr)\epsilon \int_S dxdy C^{-1-\epsilon}x(1-x-y+2xy) \tag{26}$$

$$\Delta i_{21} = 8B^-(qr)\epsilon \int_S dxdy C^{-1-\epsilon}xy(1-2y) \tag{27}$$

where C, $C^{-1-\epsilon}$, and $B^\pm$ are given by

$$C = m_c^2 - 2xy(qr) - x(1-x)r^2 - i\delta$$

$$C^{-1-\epsilon} = -\exp(i\pi\epsilon)[x(1-x)]^{-1-\epsilon} \times \left[r^2 + \frac{2y(qr)}{1-x} - \frac{m_c^2}{x(1-x)} + i\delta\right]^{-1-\epsilon} \tag{28}$$

$$B^+ = (1+\epsilon)\Gamma(\epsilon)\exp(\gamma_E\epsilon)\mu^{2\epsilon},$$

$$B^- = (\epsilon-1)\Gamma(\epsilon)\exp(\gamma_E\epsilon)\mu^{2\epsilon}. \tag{29}$$

The range of integration in (x,y) is restricted to the simplex S, i.e., $0 \leqslant y \leqslant (1-x)$ and $0 \leqslant x \leqslant 1$.

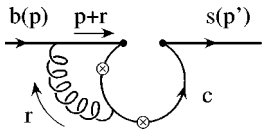

FIG. 3. Feynman diagram for the Mellin-Barnes example. The momentum and the polarization vector of the emitted gluon are denoted by q and ε, respectively.

We are now ready to evaluate the two-loop diagrams. Because of the absence of extra singularities in the limit of vanishing strange quark mass, we set $m_s = 0$ from the very beginning.

In Ref. [24] the detailed calculation of one of the diagrams in Fig. 1(a) was presented for $b \to s\gamma$. As all the other diagrams, which involve the building block I_β, i.e., (a), (b), (e), and (f) in Fig. 1, can be computed in a very similar way, we prefer to concentrate on the diagrams involving the building block $J_{\alpha\beta}$. As an example in this class, we concentrate on the diagrams (d) in Fig. 1, which we redisplay in Fig. 3 in order to set up the notation for the momenta.

The sum $\hat{M}_2(d)$ of the two diagrams can be decomposed into a color symmetric part $\hat{M}_2^+(d)$ and a color antisymmetric part $\hat{M}_2^-(d)$ according to

$$\hat{M}_2(d) = \hat{M}_2^+(d) + \hat{M}_2^-(d), \tag{30}$$

with

$$\hat{M}_2^-(d) = g_s(-i)f^{ABC}T^BT^C\mu^{2\epsilon}\frac{e^{\epsilon\gamma_E}}{(4\pi)^\epsilon}\frac{1}{i}\int\frac{d^dr}{(2\pi)^d}\overline{u}(p') \times (T^-_{\alpha\beta}\varepsilon^\alpha)\frac{\not p + \not r + m_b}{r^2 + 2(pr)}\gamma^\beta u(p)\frac{1}{r^2}$$

$$\hat{M}_2^+(d) = g_s\frac{3}{2}T^A\mu^{2\epsilon}\frac{e^{\epsilon\gamma_E}}{(4\pi)^\epsilon}\frac{1}{i}\int\frac{d^dr}{(2\pi)^d}\overline{u}(p') \times (T^+_{\alpha\beta}\varepsilon^\alpha)\frac{\not p + \not r + m_b}{r^2 + 2(pr)}\gamma^\beta u(p)\frac{1}{r^2}, \tag{31}$$

where $T^+_{\alpha\beta}$ and $T^-_{\alpha\beta}$ are given in Eqs. (12) and (13), respectively. As the calculation of $\hat{M}_2^+(d)$ is nothing but a repetition of the $b \to s\gamma$ case, we concentrate on $\hat{M}_2^-(d)$ in the following. All the Δi quantities in $T^-_{\alpha\beta}$ contain the factor $C^{-1-\epsilon}$, whose explicit form is given in Eq. (28). $\hat{M}_2^-(d)$ can be written in the form

$$\hat{M}_2^-(d) = \frac{g_s^3}{32\pi^2}(-i)f^{ABC}T^BT^C\mu^{2\epsilon}\frac{e^{\epsilon\gamma_E}}{(4\pi)^\epsilon}\frac{1}{i} \times \int\frac{d^dr}{(2\pi)^d}\overline{u}(p')P(r)u(p) \times \frac{[-\exp(i\pi\epsilon)][x(1-x)]^{-1-\epsilon}}{D_1D_2D_3^{1+\epsilon}}, \tag{32}$$

with $D_1=(r^2+2(pr))$, $D_2=r^2$, $D_3=r^2+2(qr)y/(1-x)-m_c^2/(x(1-x))$. The symbol $P(r)$ is a matrix in Dirac space, which depends in a polynomial way on the integration variable r. In the next step, the three propagators D_1, D_2, and D_3 in the denominator are Feynman parametrized as

$$\frac{1}{D_1 D_2 D_3^{1+\epsilon}}=\frac{\Gamma(3+\epsilon)}{\Gamma(1+\epsilon)}\int_S \frac{dudww^\epsilon}{[r^2+2(pr)u+2(qr)yw/(1-x)-m_c^2 w/(x(1-x))+i\delta]^{3+\epsilon}} \tag{33}$$

with $0\leqslant w\leqslant 1-u$ and $0\leqslant u\leqslant 1$. Then the integral over the loop momentum r is performed. At this level, a four dimensional integral over the Feynman parameters $(x,y;u,w)$ remains. It is useful for the following to perform the substitutions

$$x\to x';\quad y\to -\frac{(1-x')(1-w'-y')}{w'};$$

$$u\to(1-w')u';\quad w\to u'w'. \tag{34}$$

The new variables then run in the intervals

$$x',u',w'\in[0,1];\quad y\in[1-w',1]. \tag{35}$$

Taking into account the corresponding Jacobian and omitting the primes ($'$) of the integration variables, $\hat{M}_2^-(d)$ can be cast into the form

$$\hat{M}_2^-(d)=\frac{g_s^3}{32\pi^2}(-i)f^{ABC}T^BT^C\int dxdydudw\bar{u}(p')\times\left[F_1\frac{\bar{C}}{\bar{C}^{2\epsilon}}+F_2\frac{1}{\bar{C}^{2\epsilon}}+F_3\frac{1}{\bar{C}^{1+2\epsilon}}\right]u(p), \tag{36}$$

where F_1, F_2, and F_3 are matrices in Dirac space depending on the Feynman parameters x, y, u, w. Note that this expression is understood to be written in such a way that F_1, F_2, and F_3 are independent of m_c. The charm quark mass then only enters through $\bar{C}$, which reads

$$\bar{C}=m_b^2uy(1-w)+\frac{m_c^2}{x(1-x)}w. \tag{37}$$

In what follows, the ultraviolet ϵ regulator remains a fixed, small positive number.

The central point of our procedure is to use now the Mellin-Barnes representation of the denominators that look like propagators $(1/(k^2-M^2)^\lambda)$ [25], which is given by $(\lambda>0)$

$$\frac{1}{(k^2-M^2)^\lambda}=\frac{1}{(k^2)^\lambda}\frac{1}{\Gamma(\lambda)}\frac{1}{2\pi i}\times\int_\gamma ds(-M^2/k^2)^s\Gamma(-s)\Gamma(\lambda+s). \tag{38}$$

The symbol γ denotes the integration path which is parallel to the imaginary axis (in the complex s-plane) hitting the real axis somewhere between $-\lambda$ and 0. In this formula, the ''momentum squared'' k^2 is understood to have a small positive imaginary part.

In our approach, we use formula (38) in order to simplify the remaining Feynman parameter integrals in Eq. (36) where we represent the factors $1/\bar{C}^{2\epsilon}$ and $1/\bar{C}^{1+2\epsilon}$ as Mellin-Barnes integrals using the identifications

$$k^2\leftrightarrow m_b^2uy(1-w);\quad M^2\leftrightarrow\frac{-m_c^2w}{x(1-x)}. \tag{39}$$

By interchanging the order of integration, we first carry out the integrals over the Feynman parameters for any given fixed value of s on the integration path γ. These integrals are basically the same as for the massless case $m_c=0$ [in Eqs. (36) and (37)] up to the factor

$$\left[\frac{w}{uy(1-w)x(1-x)}\right]^s\left(\frac{m_c^2}{m_b^2}\right)^s. \tag{40}$$

Note that the functions F_1, F_2, and F_3 are such that the Feynman parameter integrals exist if the integration path γ is properly chosen. In the terms involving F_2 and F_3 in Eq. (36), the path must be chosen such that $-\epsilon<\mathrm{Re}(s)<0$; in the terms involving F_1 the situation is slightly more complicated: $\bar{C}$ in the numerator should be replaced by the right-hand side (RHS) of Eq. (37). For the terms proportional to m_b^2 the path has to be chosen as for the F_2 and F_3 contributions. The terms proportional to m_c^2, however, lead to Feynman parameter integrals which do not converge for values of s on this path. It turns out that the path has to be chosen such that $-2\epsilon<\mathrm{Re}(s)<-\epsilon$ in order to have convergent integrals for these terms.

We would like to mention that the variable substitutions in Eq. (34) were constructed in such a way that all the Feynman parameter integrals are either elementary or of the form $\int_0^1 dx x^p(1-x)^q=\beta(p+1,q+1)$.

For the s integration we use the residue theorem after closing the integration path in the right s-halfplane. According to the above discussion, the residue at $s=-\epsilon$ has to be taken into account in the terms proportional to m_c^2. In the other terms, however, the residue at $s=-\epsilon$ must not be taken into account. The other poles inside the integration contour are located at

$$
\begin{aligned}
&s=0,1,2,3,\ldots\\
&s=1-\epsilon,2-\epsilon,3-\epsilon,\ldots\\
&s=1-2\epsilon,2-2\epsilon,3-2\epsilon,\ldots\\
&s=1/2-2\epsilon,3/2-2\epsilon,5/2-2\epsilon,\ldots\\
&s=1-3\epsilon,2-3\epsilon,3-3\epsilon,\ldots.
\end{aligned}
\tag{41}
$$

The other two-loop diagrams are evaluated similarly. The non-trivial Feynman integrals can always be reduced to β-functions after suitable substitutions.

The sum over the residues naturally leads to an expansion in $z=(m_c^2/m_b^2)$ through the factor $(m_c^2/m_b^2)^s$ in Eq. (40). This expansion, however, is not a Taylor series; it also involves logarithms of z, which are generated by the expansion in ϵ. A generic diagram which we denote by G has then the form

$$
G=c_0+\sum_{n,m} c_{nm} z^n \ln^m z, \quad z=\frac{m_c^2}{m_b^2}. \tag{42}
$$

The power n in Eq. (42) is in general a natural multiple of 1/2 and m is a natural number including 0. In the explicit calculation, the lowest n turns out to be $n=1$. This implies the important fact that the limit $m_c \to 0$ exists.

From the structure of the poles one can see that the power m of the logarithm is bounded by 4, independent of the value of n. For a detailed explanation, we refer to [24]. As in this reference, we retain all terms up to $n=3$ in our results.

Unlike in $b\to s\gamma$, the diagrams in the individual figures are not gauge invariant. This statement holds even for the sum of all the diagrams in (a)–(f) in Fig. 1. A gauge invariant result is only obtained after including the diagrams in (g) and (h).[3] We would like to mention that the diagrams analogous to (g) also exist for $b\to s\gamma$. Their sum, however, vanishes in this case. As there are no gauge invariant subsets, we only present the result which is obtained by summing all diagrams (a)–(h) in Fig. 1. The result for $\hat{M}_2=\langle sg|\hat{O}_2|b\rangle$ reads [using $z=(m_c/m_b)^2$ and $L=\ln z$]

$$
\begin{aligned}
\hat{M}_2=&\frac{1}{2592}\frac{\alpha_s}{\pi}\langle sg|O_8|b\rangle_{\text{tree}}\left(\frac{m_b}{\mu}\right)^{-4\epsilon}\Bigg\{-\frac{384}{\epsilon}-2170-54\pi^2+z[48816-252\pi^2+(22680-1620\pi^2)L+2808L^2+612L^3\\
&-6480\zeta(3)]-12672\pi^2 z^{3/2}+z^2[66339+1872\pi^2+(-40446+1512\pi^2)L+6642L^2-1008L^3+7776\zeta(3)]\\
&+z^3[-3420-60\pi^2-6456L+7884L^2]+24\pi i[-28+z(549-24\pi^2+153L+72L^2)\\
&+z^2(-432+30\pi^2+54L-90L^2)+z^3(-259+192L)]\Bigg\}.
\end{aligned}
\tag{43}
$$

In this expression, the symbol ζ denotes the Riemann Zeta function, with $\zeta(3)\approx 1.2021$; The symbol $\langle sg|O_8|b\rangle_{\text{tree}}$ denotes the tree level matrix element of the operator O_8. As such, it contains the running b-quark mass and the running strong coupling constant, both evaluated at the scale μ [see Eq. (4)]. However, as the corrections to O_2 are explicitly proportional to α_s, we are allowed (modulo higher order terms) to identify the running b-quark mass with the pole mass m_b; in the same spirit we can identify the strong coupling constant with $g_s(m_b)$. With this interpretation, which we will use in the following, $\langle sg|O_8|b\rangle_{\text{tree}}$ is a scale independent quantity, reading

$$
\langle sg|O_8|b\rangle_{\text{tree}}=m_b\frac{g_s(m_b)}{8\pi^2}\overline{u}(p')\not{\epsilon}\not{q}RT^A u(p). \tag{44}
$$

We now turn to the matrix elements of the operator $\hat{O}_1$. Due to the specific color structure it is straightforward to see that only the diagrams (e) and (f) in Fig 1 yield a non-vanishing contribution, which is generated by the color symmetric part of the building block $J_{\alpha\beta}$ in Eq. (11). The complete regularized result for $\hat{M}_1=\langle sg|\hat{O}_1|b\rangle$ reads

$$
\begin{aligned}
\hat{M}_1=&\frac{1}{96}\frac{\alpha_s}{\pi}\langle sg|O_8|b\rangle_{\text{tree}}\left(\frac{m_b}{\mu}\right)^{-4\epsilon}\Bigg\{-\frac{18}{\epsilon}-87+z[120-16\pi^2+(120-36\pi^2)L+12L^2+4L^3-144\zeta(3)]\\
&+z^2[84+32\pi^2-24\pi^2 L-12L^2+4L^3]+z^3[-56-12\pi^2+96L-36L^2]-4\pi i[3+z(-24+2\pi^2-6L-6L^2)\\
&+z^2(-6+2\pi^2+12L-6L^2)-12z^3]\Bigg\}.
\end{aligned}
\tag{45}
$$

[3]We thank M. Neubert for making us aware of these diagrams.

The regularized matrix elements M_1 and M_2 of O_1 and O_2 in the operator basis (4) are related to $\hat{M}_1$ in Eq. (45) and $\hat{M}_2$ in Eq. (43) as follows:

$$M_1 = \tfrac{1}{2}\hat{M}_1 - \tfrac{1}{6}\hat{M}_2; \quad M_2 = \hat{M}_2. \tag{46}$$

B. Counterterms to the O_1 and O_2 contributions

The operators mix under renormalization and thus the counterterm contributions must be taken into account. As we are interested in this section in contributions to $b \to sg$ which are proportional to C_1 and C_2, we have to include, in addition to the two-loop matrix elements of C_1O_1 and C_2O_2, also the one-loop matrix elements of the four Fermi operators $C_i \delta Z_{ij} O_j (i=1,2; j=1,\ldots,6)$ and the tree level contribution of the magnetic operator $C_i \delta Z_{i8} O_8$ $(i=1,2)$. In the NDR scheme the only non-vanishing contributions to $b \to sg$ come from $j=4,8$ only. The operator renormalization constants Z_{ij} are obtained from the leading order anomalous dimension matrix in the literature [19].[4] The entries needed in our calculation are

$$\delta Z_{14} = -\frac{\alpha_s}{36\pi\epsilon}, \quad \delta Z_{18} = \frac{167\alpha_s}{2592\pi\epsilon}. \tag{47}$$

$$\delta Z_{24} = \frac{\alpha_s}{6\pi\epsilon}, \quad \delta Z_{28} = \frac{19\alpha_s}{108\pi\epsilon}. \tag{48}$$

The counterterm contributions $M_1^{\rm ct}$ and $M_2^{\rm ct}$ proportional to C_1 and C_2 are then given by

$$M_1^{\rm ct} = \langle sg | \delta Z_{14} O_4 + \delta Z_{18} O_8 | b \rangle = \left(\frac{\alpha_s}{216\pi} \frac{1}{\epsilon} \left(\frac{m_b}{\mu} \right)^{-2\epsilon} + \frac{\alpha_s}{\pi} \frac{167}{2592} \frac{1}{\epsilon} \right) \langle sg | O_8 | b \rangle_{\rm tree}. \tag{49}$$

$$M_2^{\rm ct} = \langle sg | \delta Z_{24} O_4 + \delta Z_{28} O_8 | b \rangle = \left(-\frac{\alpha_s}{36\pi} \frac{1}{\epsilon} \left(\frac{m_b}{\mu} \right)^{-2\epsilon} + \frac{\alpha_s}{\pi} \frac{19}{108} \frac{1}{\epsilon} \right) \langle sg | O_8 | b \rangle_{\rm tree}. \tag{50}$$

We note that there are no one-loop contributions to the matrix element for $b \to sg$ from the counterterms proportional to the evanescent operators P_{11} and P_{12} given in Appendix A of Ref. [19].

C. Renormalized matrix elements of O_1 and O_2

Adding the regularized two-loop result in Eq. (43) and the counterterm in Eq. (50), we find the renormalized result for M_2 in the NDR scheme:

$$M_2^{\rm ren} = \langle sg | O_8 | b \rangle_{\rm tree} \frac{\alpha_s}{4\pi} \left(l_2 \ln \frac{m_b}{\mu} + r_2 \right), \tag{51}$$

with

$$l_2 = \frac{70}{27} \tag{52}$$

$$\begin{aligned} \mathrm{Re}(r_2) = \frac{1}{648}\{ & -2170 - 54\pi^2 + z[48\,816 - 252\pi^2 \\ & + (22\,680 - 1620\pi^2)L + 2808L^2 + 612L^3 \\ & - 6480\zeta(3)] - 12\,672\pi^2 z^{3/2} + z^2[66\,339 + 1872\pi^2 \\ & + (-40\,446 + 1512\pi^2)L + 6642L^2 - 1008L^3 \\ & + 7776\zeta(3)] + z^3[-3420 - 60\pi^2 - 6456L \\ & + 7884L^2]\} \end{aligned}$$

$$\begin{aligned} \mathrm{Im}(r_2) = \frac{\pi}{27}\{ & -28 + z[549 - 24\pi^2 + 153L + 72L^2] \\ & + z^2[-432 + 30\pi^2 + 54L - 90L^2] \\ & + z^3[-259 + 192L]\}. \end{aligned} \tag{53}$$

Here, $\mathrm{Re}(r_2)$ and $\mathrm{Im}(r_2)$ denote the real and the imaginary part of r_2, respectively. The quantity z is defined as $z = (m_c^2/m_b^2)$ and $L = \ln(z)$.

Similarly, we obtain the renormalized version of M_1 by adding the regularized two-loop result in Eq. (46) and the counterterm in Eq. (49); we find

$$M_1^{\rm ren} = \langle sg | O_8 | b \rangle_{\rm tree} \frac{\alpha_s}{4\pi} \left(l_1 \ln \frac{m_b}{\mu} + r_1 \right), \tag{54}$$

with

$$l_1 = \frac{173}{162} \tag{55}$$

$$\begin{aligned} \mathrm{Re}(r_1) = -\frac{1}{3888}\{ & 4877 - 54\pi^2 + 36z[1086 + 29\pi^2 \\ & + (360 + 36\pi^2)L + 51L^2 + 8L^3 + 144\zeta(3)] \\ & - 12\,672\pi^2 z^{3/2} + 9z^2[6615 - 80\pi^2 \\ & + (-4494 + 384\pi^2)L + 864L^2 - 148L^3 + 864\zeta(3)] \\ & + 12z^3[93 + 76\pi^2 - 1186L + 900L^2]\} \end{aligned}$$

$$\begin{aligned} \mathrm{Im}(r_1) = -\frac{\pi}{324}\{ & 25 + 6z[75 + \pi^2 + 24L - 3L^2] \\ & + 6z^2[-171 + 19\pi^2 + 72L - 57L^2] \\ & + 2z^3[-421 + 192L]\}. \end{aligned} \tag{56}$$

In Figs. 4 and 5 we show the real and the imaginary parts of r_2 and r_1, respectively. For $z \geqslant 1/4$ the imaginary parts must

[4] Note that the effective anomalous dimension matrix $\gamma^{0,\rm eff}$ given in [19] has to be converted into γ^0, before the relevant δZ-factors can be read off.

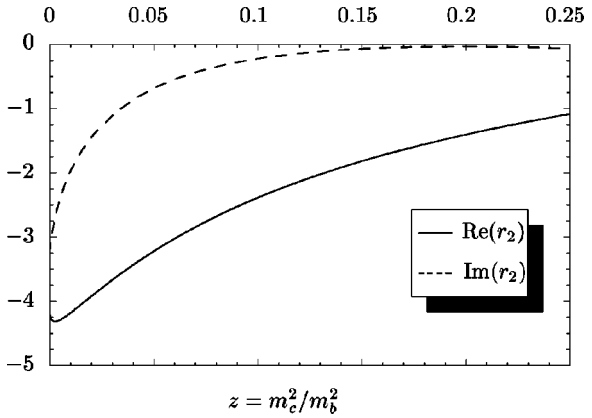

FIG. 4. Real and imaginary part of r_2 in the NDR scheme [from Eq. (53)].

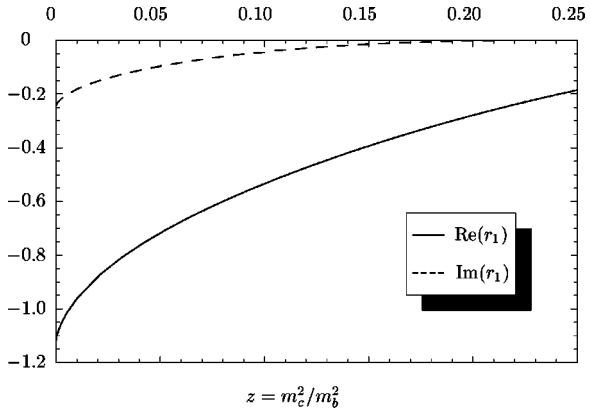

FIG. 5. Real and imaginary part of r_1 in the NDR scheme [from Eq. (56)].

vanish exactly; indeed we see from these plots that the imaginary parts based on the expansion retaining terms up to z^3 indeed vanish at $z=1/4$ to high accuracy.

IV. VIRTUAL CORRECTIONS TO O_8

In this section we calculate the order α_s virtual corrections to the matrix element

$$M_8 = \langle sg|O_8|b\rangle. \tag{57}$$

As the contributing Feynman graphs in Fig. 6 are one loop diagrams, the computation of M_8 is straightforward. We use dimensional regularization for both, the ultraviolet and the infrared singularities. Singularities which appear in the situation where the virtual gluon becomes almost real and collinear with the emitted gluon are also regulated dimensionally; on the other hand, those singularities where the almost real internal gluon is collinear with the *s*-quark, are regulated with a small strange quark mass m_s; the latter manifest themselves in logarithmic terms of the form $\ln(\rho)$, where $\rho = (m_s/m_b)^2$.

We were able to separate the ultraviolet $1/\epsilon$ poles from those which are of infrared (and/or collinear) origin. For ultraviolet poles we use the symbol $1/\epsilon$ in the following, while collinear and infrared poles are denoted by $1/\epsilon_{\rm IR}$.

When working in Feynman gauge for the gluon propagator, the individual diagrams contributing to M_8 have the following infrared and collinear properties (the letters refer to the diagrams in Fig. 6): (a) and (b) are free of infrared and collinear singularities; (c) has combined infrared and collinear singularities of the form $1/\epsilon_{\rm IR}^2$ or $\ln(\rho)/\epsilon_{\rm IR}$ as well as $1/\epsilon_{\rm IR}$ poles; (d) has combined infrared and collinear singularities of the form $1/\epsilon_{\rm IR}^2$ as well as $1/\epsilon_{\rm IR}$ poles; (e) has a collinear singularity of the form $\ln(\rho)$; (f) is free of infrared and collinear singularities; (g) has a combined collinear and infrared singularity of the form $\ln(\rho)/\epsilon_{\rm IR}$ as well as collinear singularities of the form $\ln^2(\rho)$ and $\ln(\rho)$; (h) has an infrared singularity of the form $1/\epsilon_{\rm IR}$; more precisely, this diagram is proportional to the combination $(1/\epsilon - 1/\epsilon_{\rm IR})$.

As the results of the individual diagrams are not very instructive, we only give their sum:

$$M_8 = \frac{\alpha_s}{4\pi} f_8 \langle sg|O_8|b\rangle_{\rm tree}, \tag{58}$$

with

$$f_8 = \left[-\frac{3}{\epsilon_{\rm IR}^2} - \frac{(4\ln(\rho)+9+9i\pi)}{3\epsilon_{\rm IR}} + \frac{11}{3\epsilon}\right]\left(\frac{m_b}{\mu}\right)^{-2\epsilon} + \frac{1}{3}\left[\frac{59\pi^2}{12} + 1 - 8\ln(\rho) + 2\ln^2(\rho) - 8i\pi\right]. \tag{59}$$

We would like to mention that we did not include diagrams with self energy insertions in the external legs. As we work in an on-shell renormalization scheme with respect to quark and gluon fields, such diagrams are cancelled against counterterm contributions.

A. Counterterms to the O_8 contribution

The counterterm is generated by expressing the bare quantities in the tree-level matrix element of O_8 by their renormalized counterparts. It has the structure

$$M_8^{\rm ct} = \delta R \langle sg|O_8|b\rangle_{\rm tree}, \tag{60}$$

where the factor δR is given by

$$\delta R = \sqrt{Z_2(m_b)}\sqrt{Z_2(m_s)}\sqrt{Z_3} Z_{g_s} Z_{m_b} Z_{88} - 1. \tag{61}$$

$Z_2(m_b)$, $Z_2(m_s)$, and Z_3 denote the on-shell wave function renormalization factors of the *b*-quark, the *s*-quark and the gluon, respectively. Z_{g_s} and Z_{m_b} denote the $\overline{\rm MS}$ renormalization constants for the strong coupling constant g_s and the *b*-quark mass factor, which appear explicitly in the definition of the operators [see Eq. (4)]. Finally, Z_{88} is the renormalization factor of the operator O_8.

The explicit form of $Z_2(m)$ reads

$$Z_2(m) = 1 - \frac{\alpha_s}{3\pi}\left(\frac{m}{\mu}\right)^{-2\epsilon}\left[\frac{1}{\epsilon} + \frac{2}{\epsilon_{\rm IR}} + 4\right] \tag{62}$$

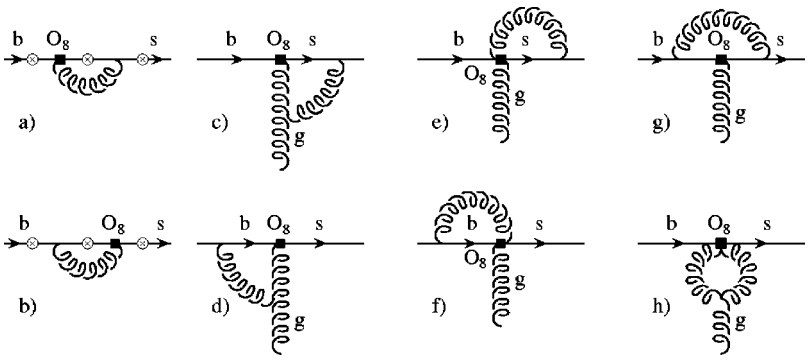

FIG. 6. Diagrams associated with the operator O_8. The real gluon can be attached to any of the circle-crosses on the fermion lines.

where we again separated infrared and ultraviolet poles. For Z_3 we get in the on-shell scheme

$$Z_3=1+\frac{\alpha_s}{2\pi}\frac{5}{2}\left(\frac{1}{\epsilon}-\frac{1}{\epsilon_{\rm IR}}\right)-\frac{\alpha_s}{2\pi}\frac{1}{3}\sum_f\left[\frac{1}{\epsilon}-2\ln\frac{m_f}{\mu}\right]. \tag{63}$$

The sum in this formula run over the five flavors $f=u,d,c,s,b$. For Z_{m_b} and Z_{88} (see Ref. [19]) one obtains

$$Z_{m_b}=1-\frac{\alpha_s}{4\pi}\frac{4}{\epsilon};\quad Z_{88}=1+\frac{\alpha_s}{4\pi}\frac{14}{3\epsilon}. \tag{64}$$

Finally, the renormalization constant for the strong coupling constant reads

$$Z_{g_s}=1-\frac{\alpha_s}{4\pi}\left[\frac{11}{2}-\frac{N_f}{3}\right]\frac{1}{\epsilon};\quad N_f=5. \tag{65}$$

Inserting the various Z factors in Eq. (61), one obtains

$$\delta R=-\frac{\alpha_s}{4\pi}\left[\frac{11}{3\epsilon}+\frac{31}{6\epsilon_{\rm IR}}-8\ln\frac{m_b}{\mu}-\frac{2}{3}\sum_f\ln\frac{m_f}{\mu}+\frac{16}{3}-2\ln\rho\right]. \tag{66}$$

B. Renormalized matrix element of O_8

Adding the regularized matrix element of O_8 in Eq. (58) and the counterterm contribution $M_8^{\rm ct}$ in Eq. (60), one obtains the renormalized result

$$M_8^{\rm ren}=\frac{\alpha_s}{4\pi}f_8^{\rm ren}\langle sg|O_8|b\rangle_{\rm tree}, \tag{67}$$

with

$$f_8^{\rm ren}=\left[-\frac{3}{\epsilon_{\rm IR}^2}-\frac{(8\ln(\rho)+49+18i\pi)}{6\epsilon_{\rm IR}}\right]\left(\frac{m_b}{\mu}\right)^{-2\epsilon}-\frac{29}{3}\ln\frac{m_b}{\mu}+\frac{2}{3}\sum_f\ln\frac{m_f}{\mu}-5+\frac{59\pi^2}{36}-\frac{2}{3}\ln\rho+\frac{2}{3}\ln^2\rho-\frac{8}{3}i\pi. \tag{68}$$

In Eq. (68) the sum runs over the five flavors $f=u,d,c,s,b$, and $\rho=(m_s/m_b)^2$. We anticipate that the singular terms of the form $1/\epsilon_{\rm IR}^2$, $1/\epsilon_{\rm IR}$ and $\ln\rho$ in Eq. (68) will cancel (at the level of the decay width) against the corresponding singularities present in the gluon bremsstrahlung corrections to $b\to sg$. On the other hand, the logarithmic terms $\ln(m_f/\mu)$, which also represent some kind of singularities for the light flavor $f=u,d,s$ are not cancelled by the gluon bremsstrahlung process. Keeping in mind that these terms originate from the renormalization factor Z_3 of the gluon field, i.e., from gluon self energy diagrams in which these flavors propagate, it is expected that these logarithms will cancel against the logarithms present in the decay rate $\Gamma(b\to sf\bar{f})$ with $f=u,d,s$. We will discuss this issue in more detail at the end of the next section.

V. VIRTUAL CORRECTIONS TO THE DECAY WIDTH FOR $b\to sg$

We are now ready to write down the renormalized version of the matrix $M^{\rm ren}(b\to sg)$ element for $b\to sg$, where the virtual order α_s corrections are included. We obtain

$$M^{\rm ren}(b\to sg)=\frac{4G_F i}{\sqrt{2}}V_{ts}^*V_{tb}\left\{C_8^{\rm eff}+\frac{\alpha_s}{4\pi}\left[C_1^0\left(l_1\ln\frac{m_b}{\mu}+r_1\right)+C_2^0\left(l_2\ln\frac{m_b}{\mu}+r_2\right)+C_8^{0,\rm eff}f_8^{\rm ren}\right]\right\}\times\langle sg|O_8(\mu)|b\rangle_{\rm tree}. \tag{69}$$

The quantities l_1, r_1, l_2, r_2, and $f_8^{\rm ren}$ are given in Eqs. (55), (56), (52), (53), and (68), respectively. As Eq. (69) shows, $C_8^{\rm eff}$ is the only Wilson coefficient needed to NLL precision. For the following, it is useful to decompose it as

$$C_8^{\rm eff}=C_8^{0,\rm eff}+\frac{\alpha_s}{4\pi}C_8^{1,\rm eff}. \tag{70}$$

The symbol $\langle sg|O_8(\mu)|b\rangle_{\rm tree}$ in Eq. (69) denotes the tree level matrix element of $O_8(\mu)$, which contains the running b-quarks mass and the strong running coupling constant at the scale μ. In order to get expressions where the b-quark mass enters as the pole mass, and the strong coupling constant enters as $g_s(m_b)$, we rewrite $\langle sg|O_8(\mu)|b\rangle_{\rm tree}$ as

$$\langle sg|O_8(\mu)|b\rangle_{\rm tree}=\langle sg|O_8|b\rangle_{\rm tree}\Bigg[1+\frac{2\alpha_s}{\pi}\ln\frac{m_b}{\mu}-\frac{4}{3}\frac{\alpha_s}{\pi}+\frac{\alpha_s}{4\pi}\beta_0\ln\frac{m_b}{\mu}\Bigg];\quad \beta_0=\frac{23}{3},\tag{71}$$

where we made use of Eqs. (5) and (A18). The symbol $\langle sg|O_8|b\rangle_{\rm tree}$ then stands for the tree level matrix element of O_8 in which $\overline{m}_b(\mu)$ and g_s have to to be identified with the pole mass m_b and $g_s(m_b)$, respectively. [See also the discussion after Eq. (43) and Eq. (44)]. Inserting Eqs. (70) and (71) into Eq. (69) we obtain

$$M^{\rm ren}(b\to sg)=\frac{4G_F i}{\sqrt{2}}V_{ts}^*V_{tb}\Bigg\{C_8^{0,\rm eff}+\frac{\alpha_s}{4\pi}\Bigg[C_8^{1,\rm eff}+(8+\beta_0)\ln\frac{m_b}{\mu}C_8^{0,\rm eff}-\frac{16}{3}C_8^{0,\rm eff}+C_1^0\Big(l_1\ln\frac{m_b}{\mu}+r_1\Big)+C_2^0\Big(l_2\ln\frac{m_b}{\mu}+r_2\Big)+C_8^{0,\rm eff}f_8^{\rm ren}\Bigg]\Bigg\}\langle sg|O_8|b\rangle_{\rm tree}.\tag{72}$$

To obtain the decay width $\Gamma^{\rm virt}$ from $M^{\rm ren}(b\to sg)$ is straightforward. We get

$$\Gamma^{\rm virt}=\frac{\alpha_s(m_b)m_b^5}{24\pi^4}|G_FV_{ts}^*V_{tb}|^2\Bigg\{(C_8^{0,\rm eff})^2+\frac{\alpha_s}{4\pi}C_8^{0,\rm eff}\times\Bigg[2C_8^{1,\rm eff}+2(8+\beta_0)\ln\frac{m_b}{\mu}C_8^{0,\rm eff}-\frac{32}{3}C_8^{0,\rm eff}+2C_1^0\Big(l_1\ln\frac{m_b}{\mu}+{\rm Re}(r_1)\Big)+2C_2^0\Big(l_2\ln\frac{m_b}{\mu}+{\rm Re}(r_2)\Big)+2C_8^{0,\rm eff}{\rm Re}(f_8^{\rm ren})(1-\epsilon)\Big(\frac{m_b}{\mu}\Big)^{-2\epsilon}\times\Big(1+2\epsilon-\frac{1}{4}(\pi^2-16)\epsilon^2\Big)\Bigg]\Bigg\}.\tag{73}$$

We note that due to the infrared poles present in $f_8^{\rm ren}$ the phase space integrations have been done consistently in $d=4-2\epsilon$ dimensions, which leads to the last two extra factors in the last term in Eq. (73). The other factor, $(1-\epsilon)$, in the last term in Eq. (73), is due to the fact that all the $(d-2)$ possible transverse polarizations of the emitted gluon were taken into account.

We already mentioned that the infrared singularities $(1/\epsilon_{\rm IR}^2,\ 1/\epsilon_{\rm IR})$ and the collinear singularities $(\ln^2\rho,\ln\rho)$ in $f_8^{\rm ren}$ in Eq. (73) cancel when adding gluon bremsstrahlung. On the other hand, the unphysical logarithms of the form $\ln(m_f/\mu)$ in $f_8^{\rm ren}$ cancel against the O_8 contribution to the decay width for $b\to s\overline{f}f$.

The appearance of these singularities signals that individually the processes $b\to sg$, $b\to sgg$, and $b\to s\overline{f}f$ are not well defined even within perturbation theory; only their sum, the inclusive charmless hadronic decay width is a well-defined physical quantity, as already discussed in the Introduction.

Keeping in mind that the ultimate goal for the future should be a complete $O(\alpha_s^2)$ calculation for the charmless hadronic decay width, we decided to add the O_8 contribution $\Gamma_8(b\to s\overline{f}f)$ to $\Gamma(b\to sg)+\Gamma(b\to sgg)$, in order to cancel the $\ln(m_f/\mu)$ terms. From the explicit expression

$$\Gamma_8(b\to s\overline{f}f)=\frac{m_b^5|G_FV_{ts}^*V_{tb}C_8^{0,\rm eff}|^2}{72\pi^5}\alpha_s^2\Big[\ln\frac{m_b}{2m_f}-\frac{2}{3}\Big],\tag{74}$$

one immediately sees that the mentioned logarithms indeed cancel.

We would like to mention that $\Gamma_8(b\to s\overline{f}f)$ is dominated by small values of q^2, where q is the momentum of the virtual gluon, decaying into the $\overline{f}f$-pair; therefore, it is reasonable to absorb this part of $b\to s\overline{f}f$ into $\mathcal{B}^{\rm NLL}(b\to sg)$.

Another reasonable definition for $\mathcal{B}^{\rm NLL}(b\to sg)$ would be to include the contributions of all the operators to $b\to s\overline{f}f$, but to impose kinematical cuts (e.g. on the invariant mass of the $\overline{f}f$-pair). Numerically, the difference between these two definitions for $\mathcal{B}^{\rm NLL}(b\to sg)$ are small for a reasonably small cut, because the NLL corrections are by far dominated by the virtual corrections to the O_2 contribution to $b\to sg$.

A third possibility is to totally omit $b\to s\overline{f}f$ and accepting a logarithmic dependence of the results for $\mathcal{B}^{\rm NLL}$ on the light quark masses. We checked numerically that this procedure and the one we chose differ by less than 2% when the masses m_f of the light quarks are assumed to be of order $\Lambda_{\rm QCD}$.

VI. MATRIX ELEMENTS FOR GLUON BREMSSTRAHLUNG

In this section we discuss the gluon bremsstrahlung corrections to $b\to sg$, i.e., the matrix element for the process $b\to sgg$, associated with the operators $\hat{O}_1$, $\hat{O}_2$, and O_8. For literature on the analogous corrections to $b\to s\gamma$, we refer to [26].

A. Bremsstrahlung associated with $\hat{O}_1$ and $\hat{O}_2$

We first discuss the matrix element of $\hat{O}_2$. There are two diagrams contributing; they are displayed in (d) and (e) of Fig. 7. The sum of diagram (d) and the one with the two gluons interchanged is denoted by $\overline{J}_{\alpha\beta}$. Its analytic form is obtained by putting $r^2=0$ and $r_\beta=0$ in the expression for $J_{\alpha\beta}$ in Eq. (11):

$$\overline{J}_{\alpha\beta}^{AB}=\overline{T}_{\alpha\beta}^{+}(q,r)\{T^A,T^B\}+\overline{T}_{\alpha\beta}^{-}(q,r)[T^A,T^B].\tag{75}$$

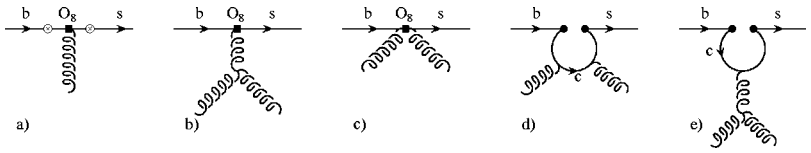

FIG. 7. Bremsstrahlung diagrams associated to O_8 and $\hat{O}_2$. Circle-crosses denote possible gluon emissions. Note that picture (a) actually represents four Feynman diagrams (obtained by interchanging the gluons) and the one in (d) represents two diagrams (again: including the interchange of the gluons).

This expression is understood to be contracted with the polarization vectors $\varepsilon^\alpha(q)$ and $\varepsilon^\beta(r)$ of the gluons. The diagram (e) in Fig. 7, denoted by $S^{AB}_{\alpha\beta}$, is color antisymmetric and can be written as

$$S^{AB}_{\alpha\beta}=S^-_{\alpha\beta}[T^A,T^B], \tag{76}$$

where $S^-_{\alpha\beta}$ reads $[t=(2qr)/m_c^2]$

$$S^-_{\alpha\beta}=\frac{g_s^2}{32\pi^2}\left[\frac{4}{3}\left(\frac{\mu}{m_c}\right)^{2\epsilon}\frac{1}{\epsilon}-\frac{4}{3}-8G_1(t)+8G_2(t)\right]$$
$$\times[\not{r}g_{\alpha\beta}-\not{q}g_{\alpha\beta}-2\gamma_\beta r_\alpha+2\gamma_\alpha q_\beta]L. \tag{77}$$

The functions $G_i(t)(i=-1,0,1,\ldots)$ are defined as

$$G_i(t)=\int_0^1 dx x^i \ln[1-tx(1-x)-i\delta]. \tag{78}$$

The Ward identities $r^\beta\overline{T}^+_{\alpha\beta}=q^\alpha\overline{T}^+_{\alpha\beta}=0$, stated in [24], imply that

$$\overline{T}^+_{\alpha\beta}=\frac{g_s^2}{32\pi^2}\left[E(\alpha,\beta,r)-E(\alpha,\beta,q)-E(\beta,r,q)\frac{r_\alpha}{(qr)}\right.$$
$$\left.+E(\alpha,r,q)\frac{q_\beta}{(qr)}\right]L\overline{\Delta i}_{23}. \tag{79}$$

General considerations (or a straightforward calculation which makes use of the explicit expressions for the functions G_i and $\overline{\Delta i}_i$) imply the Ward identities

$$r^\beta(\overline{T}^-_{\alpha\beta}+S^-_{\alpha\beta})=0; \quad q^\alpha(\overline{T}^-_{\alpha\beta}+S^-_{\alpha\beta})=0, \tag{80}$$

which can be used to cast $(\overline{T}^-_{\alpha\beta}+S^-_{\alpha\beta})$ into the simple form

$$\overline{T}^-_{\alpha\beta}+S^-_{\alpha\beta}=\frac{g_s^2}{32\pi^2}(\not{r}-\not{q})\left(\frac{r_\alpha q_\beta}{qr}-g_{\alpha\beta}\right)L\overline{\Delta i}_{17}. \tag{81}$$

To summarize, the matrix element $\hat{M}_2^{\rm brems}=\langle sgg|\hat{O}_2|b\rangle$ can be written as

$$\hat{M}_2^{\rm brems}=\overline{T}^+_{\alpha\beta}\{T^A,T^B\}+(\overline{T}^-_{\alpha\beta}+S^-_{\alpha\beta})[T^A,T^B], \tag{82}$$

where $\overline{T}^+_{\alpha\beta}$ and $(\overline{T}^-_{\alpha\beta}+S^-_{\alpha\beta})$ are given in Eqs. (79) and (81), respectively. The functions $\overline{\Delta i}_{23}$ and $\overline{\Delta i}_{17}$ occurring in these expressions, can be written in terms of $G_0(t)$ and $G_{-1}(t)$ $[t=(2qr)/m_c^2]$ defined in Eq. (78):

$$\overline{\Delta i}_{23}=-2\frac{t+2G_{-1}(t)}{t};$$

$$\overline{\Delta i}_{17}=-\frac{2}{3}\frac{t+6G_{-1}(t)-12G_0(t)}{t}. \tag{83}$$

The explicit form of $G_{-1}(t)$ and $G_0(t)$ is given in Appendix B. Note that these results are ultraviolet finite. As the subsequent phase space integrals do not generate infrared singularities, it is consistent to retain terms up to order ϵ^0 only in Eq. (82).

Due to the specific color structure of the operator $\hat{O}_1$, the diagram (e) in Fig. 7 does not contribute and the color antisymmetric part encoded in $\overline{T}^-_{\alpha\beta}$ is also absent. The matrix element $\hat{M}_1^{\rm brems}=\langle sgg|\hat{O}_1|b\rangle$ is therefore proportional to $\overline{T}^+_{\alpha\beta}$, reading

$$\hat{M}_1^{\rm brems}=\overline{T}^+_{\alpha\beta}\delta^{AB}\delta^{ab}; \tag{84}$$

A,B and a,b are the color indices of the gluons and the quarks, respectively.

B. Bremsstrahlung associated with O_8

The Feynman diagrams contributing to the matrix element $M_8^{\rm brems}=\langle sgg|O_8|b\rangle$ are shown in (a), (b), and (c) in Fig. 7. Similar to $\hat{M}_2^{\rm brems}$ in Eq. (82), one can decompose $M_8^{\rm brems}$ into a color symmetric- and a color antisymmetric part:

$$M_8^{\rm brems}=R^+_{\alpha\beta}\{T^A,T^B\}+R^-_{\alpha\beta}[T^A,T^B]. \tag{85}$$

The diagrams shown in (b) and (c) only contribute to $R^-_{\alpha\beta}$, while the diagrams in (a) contribute to both $R^-_{\alpha\beta}$ and $R^+_{\alpha\beta}$. As the calculation of these tree level diagrams is straightforward, we do not give the explicit expressions for $R^+_{\alpha\beta}$ and $R^-_{\alpha\beta}$.

VII. DECAY WIDTH FOR $b\to sgg$

The total matrix element $M^{\rm brems}(b\to sgg)$ can be written as

$$M^{\rm brems}=\frac{4G_F i}{\sqrt{2}}V^*_{ts}V_{tb}[\hat{C}_1\hat{M}_1^{\rm brems}+\hat{C}_2\hat{M}_2^{\rm brems}+C_8^{0,\rm eff}M_8^{\rm brems}], \tag{86}$$

where the three terms on the RHS, given in Eqs. (84), (82) and (85), correspond to the contributions of the operators

$\hat{O}_1$, $\hat{O}_2$, and O_8, respectively. The coefficients $\hat{C}_1$ and $\hat{C}_2$ are understood to be the following linear combinations of the Wilson coefficients C_1 and C_2 appearing in the effective Hamiltonian (3):

$$\hat{C}_1 = \tfrac{1}{2} C_1; \quad \hat{C}_2 = C_2 - \tfrac{1}{6} C_1. \tag{87}$$

We note that in Eq. (86) only the leading order pieces of the Wilson coefficients are needed.

The expression for the decay width reads in d dimensions:

$$d\Gamma^{\rm brems}(b \to s g g) = \frac{1}{2m_b} \int (2\pi)^d \delta^d(p - p' - q - r) \times \overline{|M^{\rm brems}|^2_\Sigma} d\mu(p') d\mu(q) d\mu(r), \tag{88}$$

where p, p', q, r are the four-momenta of the b-quark, s-quark, and the gluons. $\overline{|M^{\rm brems}|^2_\Sigma}$ is obtained by squaring the matrix element $M^{\rm brems}$, followed by summing (averaging) over spins and color of the final (initial) state particles. The factor (1/2) due to the two gluons in the final state is also absorbed there.

The phase space integrals are plagued with infrared and collinear singularities. Configurations with one gluon flying collinear to the s-quark are regulated by a small strange quark mass m_s, while configurations with two collinear gluons, or one soft gluon are dimensionally regularized. As in the calculations of the virtual corrections, we write the dimension as $d = 4 - 2\epsilon$. (Note that ϵ has to be negative in order to regulate the phase space integrals.)

When squaring $M^{\rm brems}$ in Eq. (86), nine terms are generated, which we denote for obvious reasons by $(\hat{O}_1, \hat{O}_1^*)$, $(\hat{O}_1, \hat{O}_2^*)$, $(\hat{O}_1, O_8^*)$, $(\hat{O}_2, \hat{O}_1^*)$, $(\hat{O}_2, \hat{O}_2^*)$, $(\hat{O}_2, O_8^*)$, $(O_8, \hat{O}_1^*)$, $(O_8, \hat{O}_2^*)$, and (O_8, O_8^*). It turns out that all terms except (O_8, O_8^*) are free of infrared and collinear singularities. We therefore can put $m_s = 0$ in these terms and evaluate the phase space integrals in $d = 4$ dimensions. Denoting this finite contribution to the decay width by $\Gamma^{\rm brems}_{\rm fin}$, we get

$$\Gamma^{\rm brems}_{\rm fin} = \frac{8 |G_F V_{ts}^* V_{tb}|^2}{64\pi^3 m_b} \frac{1}{12} \frac{\alpha_s^2}{64\pi^2} \int dE_q dE_r \times (\tau_{11}^+ + \tau_{22}^+ + \tau_{22}^- + \tau_{12}^+ + \tau_{18}^+ + \tau_{28}^+ + \tau_{28}^-). \tag{89}$$

The superscripts $(+)$ and $(-)$ on the various τ-quantities refer to color even and color odd contributions, respectively. The result is represented as a two dimensional integral over the energies E_q and E_r of the gluons in the rest frame of the b-quark. E_q and E_r vary in the range

$$E_q \in \left[0, \frac{m_b}{2}\right]; \quad E_r \in \left[\frac{m_b}{2} - E_q, \frac{m_b}{2}\right]. \tag{90}$$

The various τ-quantities, in which all the scalar products are understood to be expressed in terms of E_q and E_r, read

$$\begin{aligned}
\tau_{11}^+ &= \hat{C}_1^2 24 |\overline{\Delta i}_{23}|^2 2 m_b^2 [m_b^2 - 2(qr)] \\
\tau_{22}^+ &= \hat{C}_2^2 \tfrac{28}{3} |\overline{\Delta i}_{23}|^2 2 m_b^2 [m_b^2 - 2(qr)] \\
\tau_{22}^- &= \hat{C}_2^2 12 |\overline{\Delta i}_{17}|^2 2 [16(pq)^2 - 16(pq)(qr) - 8 m_b^2 (pq) + 6 m_b^2 (qr) + m_b^4] \\
\tau_{12}^+ &= 2 \hat{C}_1 \hat{C}_2 8 |\overline{\Delta i}_{23}|^2 2 m_b^2 [m_b^2 - 2(qr)] \\
\tau_{18}^+ &= 2 \hat{C}_1 C_8^{0,\rm eff} 8 {\rm Re}(\overline{\Delta i}_{23}) 16 m_b^2 (qr) \\
\tau_{28}^+ &= 2 \hat{C}_2 C_8^{0,\rm eff} \tfrac{28}{3} {\rm Re}(\overline{\Delta i}_{23}) 16 m_b^2 (qr) \\
\tau_{28}^- &= 2 \hat{C}_2 C_8^{0,\rm eff} 12 {\rm Re}(\overline{\Delta i}_{17}) (-4 m_b^2) [m_b^4 (pq) + m_b^4 (pr) - 2 m_b^2 (pq)^2 - 2 m_b^2 (pr)^2 \\
&\quad - 2 m_b^2 (pq)(pr) + 4 (pq)^2 (pr) + 4 (pr)^2 (pq)] / [(pq)(pr)]
\end{aligned} \tag{91}$$

were the functions $\overline{\Delta i}_{17}$ and $\overline{\Delta i}_{23}$ are given in Eq. (83). As these function are rather complicated, the integrals over E_q and E_r are done numerically.

We now turn to the (O_8, O_8^*) contribution, denoted by $\Gamma^{\rm brems}_{88}$. Without going too much into the details, we would like to mention that some care has to be taken when summing over the $(d-2)$ transverse polarizations of the gluons. These sums are of the form

$$\sum_{r=1}^{d-2} \varepsilon_r^\mu(k) \varepsilon_r^{*\nu}(k) = -g^{\mu\nu} + k^\mu f^\nu + k^\nu f^\mu, \tag{92}$$

where the vector f satisfies the condition $(fk) = 1$, with k being the four-momentum of the gluon. It turns out that both terms involving f on the RHS in Eq. (92) contribute to the color antisymmetric part of $\Gamma^{\rm brems}_{88}$. After a lengthy, but straightforward calculation, we obtain [with $\rho = (m_s/m_b)^2$]

$$\Gamma^{{\rm brems},+}_{88} = \frac{7 \alpha_s (C_8^{0,\rm eff})^2 V}{96\pi} \left(\frac{m_b}{\mu}\right)^{-4\epsilon} \times \left[\frac{8 + 4\ln\rho}{\epsilon_{\rm IR}} - 2\ln^2\rho + 6\ln\rho + 18 - \frac{4\pi^2}{3}\right] \tag{93}$$

for the color symmetric part, and

$$\Gamma^{{\rm brems},-}_{88} = \frac{\alpha_s (C_8^{0,\rm eff})^2 V}{16\pi} \left(\frac{m_b}{\mu}\right)^{-4\epsilon} \left[\frac{24}{\epsilon_{\rm IR}^2} + \frac{80 + 6\ln\rho}{\epsilon_{\rm IR}} - 3\ln^2\rho + 9\ln\rho + 299 - 26\pi^2\right] \tag{94}$$

for the color antisymmetric part. V is defined as

$$V=\frac{\alpha_s m_b^5}{24\pi^4}|G_F V_{ts}^* V_{tb}|^2. \tag{95}$$

The total decay width for $b\to sgg$ is then given by

$$\Gamma^{\rm brems}(b\to sgg)=\Gamma_{\rm fin}^{\rm brems}+\Gamma_{88}^{\rm brems,+}+\Gamma_{88}^{\rm brems,-}, \tag{96}$$

where the three terms on the RHS are given in Eqs. (89), (93), and (94).

VIII. COMBINED NLL BRANCHING RATIO FOR $b\to sg$ AND $b\to sgg$

In this section we combine the decay widths for the virtually corrected process $b\to sg$ and the bremsstrahlung process $b\to sgg$ to the decay width, which we call $\Gamma^{\rm NLL}(b\to sg)$. We also absorb in this quantity the O_8 induced contribution to the process $b\to s\bar{f}f$, where $f=u,d,s$, as discussed at the end of Sec. V. The expression for $\Gamma^{\rm virt}$, which contains the lowest order contribution to the decay width for $b\to sg$, together with its virtual corrections, may be found in Eq. (73). The result for the bremsstrahlung process, $\Gamma^{\rm brems}$ is given in Eq. (96). From the explicit formulas for $\Gamma^{\rm virt}$ and $\Gamma^{\rm brems}$ one can see that the infrared singularities and those collinear singularities, which are regulated by $\epsilon_{\rm IR}$ cancel in the sum. The same also happens with the collinear singularities which are regularized by the parameter $\rho=(m_s/m_b)^2$. The terms containing logarithms of the light quark masses m_f, present in the result for $\Gamma^{\rm virt}$, are cancelled when combined with $\Gamma_8(b\to s\bar{f}f)$ in Eq. (74). Putting together the individual pieces, we obtain

$$\begin{aligned}\Gamma^{\rm NLL}(b\to sg)=&\frac{\alpha_s(m_b)m_b^5}{24\pi^4}|G_F V_{ts}^* V_{tb}|^2\Bigg\{(C_8^{0,\rm eff})^2\\&+\frac{\alpha_s}{4\pi}C_8^{0,\rm eff}\Bigg[2C_8^{1,\rm eff}-\frac{32}{3}C_8^{0,\rm eff}+2C_1^0\\&\times\left[l_1\ln\frac{m_b}{\mu}+{\rm Re}(r_1)\right]\\&+2C_2^0\left[l_2\ln\frac{m_b}{\mu}+{\rm Re}(r_2)\right]+2C_8^{0,\rm eff}\\&\times\left[(l_8+8+\beta_0)\ln\frac{m_b}{\mu}+r_8\right]\Bigg]\Bigg\}+\Gamma_{\rm fin}^{\rm brems},\end{aligned} \tag{97}$$

where $\Gamma_{\rm fin}^{\rm brems}$, given in Eq. (89), contains all the bremsstrahlung corrections except those originating from the (O_8,O_8^*) interference. The quantities l_1, r_1, l_2, and r_2 stem from the virtual corrections; they are given in Eqs. (55), (56), (52), and (53), respectively. On the other hand, l_8 and r_8 contain information from the real part of the virtual corrections, encoded in ${\rm Re}(f_8^{\rm ren})$; the contributions from the (O_8,O_8^*) interference of the gluon bremsstrahlung process; and the O_8 contribution to the process $b\to s\bar{f}f$: The explicit expressions for l_8 and r_8 (which is real by definition) read

$$l_8=-\frac{19}{3};\quad r_8=\frac{1}{18}\left[351-19\pi^2-36\ln 2+6\ln\frac{m_c^2}{m_b^2}\right]. \tag{98}$$

We would like to stress that all scale dependent quantities in Eq. (97) are understood to be evaluated at the scale μ, unless indicated explicitly in the notation.

To prepare the discussion on the numerical size of the NLL QCD corrections, it is useful to cast the final result (97) into another form:

$$\Gamma^{\rm NLL}(b\to sg)=\frac{\alpha_s(m_b)m_b^5}{24\pi^4}|G_F V_{ts}^* V_{tb}|^2|\overline{D}|^2+\Gamma_{\rm fin}^{\rm brems}, \tag{99}$$

with

$$\begin{aligned}\overline{D}=&C_8^{0,\rm eff}+\frac{\alpha_s}{4\pi}\Bigg[C_8^{1,\rm eff}-\frac{16}{3}C_8^{0,\rm eff}+C_1^0\left[l_1\ln\frac{m_b}{\mu}+r_1\right]\\&+C_2^0\left[l_2\ln\frac{m_b}{\mu}+r_2\right]+C_8^{0,\rm eff}\left[(l_8+8+\beta_0)\ln\frac{m_b}{\mu}+r_8\right]\Bigg].\end{aligned} \tag{100}$$

The modulus square of $\overline{D}$ is understood to be taken in the same way as in the virtual contributions, i.e., by systematically discarding the $O(\alpha_s^2)$ term. In this sense, the quantity $\overline{D}$ can be viewed as an effective matrix element.

We would like to mention that l_1, l_2, and $(l_8+8+\beta_0)$ are identical to the anomalous dimension matrix elements $\gamma_{18}^{0,\rm eff}$, $\gamma_{28}^{0,\rm eff}$, and $\gamma_{88}^{0,\rm eff}$, respectively. This is of course what has to happen: Only in this case the leading scale dependence of $C_8^{0,\rm eff}(\mu)$ gets compensated by the second term in Eq. (100).

The NNL branching ratio $\mathcal{B}^{\rm NLL}(b\to sg)$ is then obtained as

$$\mathcal{B}^{\rm NLL}(b\to sg)=\frac{\Gamma^{\rm NLL}(b\to sg)}{\Gamma_{\rm sl}}\mathcal{B}_{\rm sl}^{\rm exp}, \tag{101}$$

where $\mathcal{B}_{\rm sl}^{\rm exp}$ denotes the experimental semileptonic branching ratio of the B-meson. $\Gamma_{\rm sl}$ stands for the theoretical expression of the semileptonic decay width of the B-meson. Neglecting non-perturbative corrections of the order $(\Lambda_{\rm QCD}/m_b)^2$, $\Gamma_{\rm sl}$ reads [with $x_c=(m_c/m_b)$]

$$\begin{aligned}\Gamma_{\rm sl}\approx\Gamma(b\to ce\bar{\nu}_e)=&\frac{G_F^2 m_b^5}{192\pi^3}|V_{cb}|^2 g(x_c)\\&\times\left[1+\frac{\alpha_s(\mu_b)}{2\pi}h_{\rm sl}(x_c)+O(\alpha_s^2)\right],\end{aligned} \tag{102}$$

where the phase space function $g(x_c)$ reads

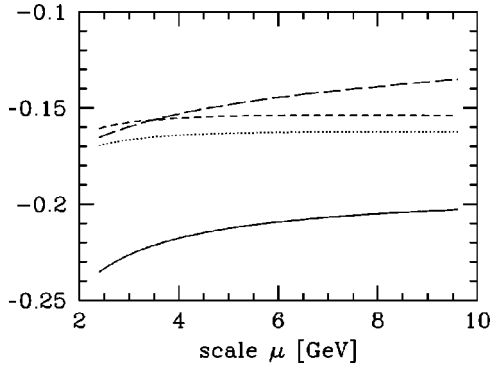

FIG. 8. Scale (μ) dependence of the function $\overline{D}$ [see Eq. (100)] in various approximations: The long-dashed line shows $C_8^{0,\mathrm{eff}}$; the short-dashed line corresponds to putting $r_1=r_2=r_8=0$; the dotted line is obtained by only putting $r_2=0$; the solid line shows the full function $\overline{D}$. See text.

$$g(x_c)=1-8x_c^2-24x_c^4\ln x_c+8x_c^6-x_c^8. \tag{103}$$

The analytic expression for $h_{\mathrm{sl}}(x_c)$ can be found in Ref. [27]. The approximation

$$h_{\mathrm{sl}}(x_c)=-3.341+4.05(x_c-0.3)-4.3(x_c-0.3)^2 \tag{104}$$

holds to an accuracy of 1 permille in the relevant range $0.2\leqslant x_c\leqslant 0.4$.

We note that in the numerical analysis of $\mathcal{B}^{\mathrm{NLL}}(b\to sg)$ we systematically expand the expression for the branching ratio (101) in α_s, dropping terms of $O(\alpha_s^2)$.

A short remark concerning the LL branching ratio is in order: For the decay width $\Gamma^{\mathrm{LL}}(b\to sg)$, we use the expression

$$\Gamma^{\mathrm{LL}}(b\to sg)=\frac{\alpha_s(\mu)m_b^5}{24\pi^4}|G_F V_{ts}^* V_{tb}|^2(C_8^{\mathrm{LL,\,eff}}(\mu))^2. \tag{105}$$

The LL branching ratio for $b\to sg$ is then obtained as in Eq. (101), but by discarding the radiative corrections in Γ_{sl}.

IX. NUMERICAL RESULTS FOR THE COMBINED BRANCHING RATIO

Before we present the numerical result for the branching ratio $\mathcal{B}^{\mathrm{NLL}}(b\to sg)$, we discuss the sizes of the various NLL corrections at the level of the function $\overline{D}$, defined in Eq. (100) [anticipating that the finite bremsstrahlung corrections in Eq. (99) are relatively small]. We already mentioned that the terms containing the explicit logarithms of the ratio (m_b/μ) get compensated by the scale dependence of the first term on the RHS of Eq. (100). This feature can be observed in Fig. 8, when comparing the two dashed lines. The long-dashed line represents only the first term C_8^0 of the function $\overline{D}$, while the short-dashed line shows $\overline{D}$, in which r_1, r_2, and r_8 are put to zero. As expected, the short-dashed line has a milder μ-dependence. When switching on also r_1 and r_8 (but keeping $r_2=0$), the resulting curve, shown by the dotted line, stays close to the short-dashed curve and the scale dependence remains mild. However, when switching on also r_2, the situation changes drastically. The resulting solid line, which represents the full NLL $\overline{D}$ function, implies that the term containing the two-loop quantity r_2, induces a large NLL correction. As this large correction term contains a factor $\alpha_s(\mu)C_2(\mu)$, it is of no surprise, that the NLL prediction for the function $\overline{D}$ suffers from a relatively large scale dependence, as illustrated by the solid line.

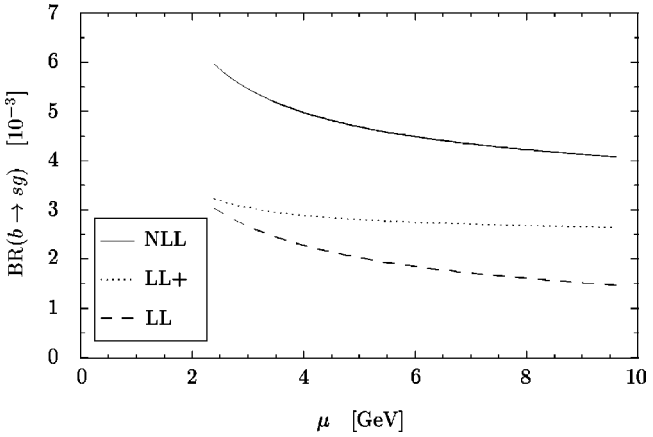

FIG. 9. Branching ratio $\mathcal{B}(b\to sg)$ as a function of the scale μ in various approximations: The dashed and the solid lines show the LL and the NLL predictions, respectively; the dotted line is obtained by putting $r_1=r_2=r_8=\Gamma_{\mathrm{brems}}^{\mathrm{fin}}=0$ in the NLL expression for $\Gamma^{\mathrm{NLL}}(b\to sg)$ in Eq. (99). See text.

The reason for the large NLL corrections in the $\overline{D}$ function can be explained as follows: At leading logarithmic precision, $\overline{D}$ only gets a contribution from the matrix element of $C_8(m_b)O_8(m_b)$; due to gauge invariance, there is no one-loop contribution of $C_2(m_b)O_2(m_b)$. The LL approximation of $\overline{D}$ is therefore given by $C_8(m_b)$, which numerically is relatively small ($|C_8(m_b)|\sim 0.15$). At the NLL order, $C_2(m_b)O_2(m_b)$ does contribute, leading to a correction $\sim(\alpha_s(m_b)/\pi)C_2(m_b)$ in the $\overline{D}$-function. The naive suppression factor $\alpha_s(m_b)/\pi$ is enhanced by an extra factor $|C_2(m_b)/C_8(m_b)|\sim 7$. In other words, the large correction is due to the absence of the O_2 contribution at LL. In this sense, a large NLL correction is not a surprise. The next-to-NLL corrections are expected to have a normal behavior [i.e., a typical suppression of the order of $\alpha_s(m_b)/\pi$ with respect to the NLL correction], because there are no operators left, which only start contributing at next-to-NLL order. We therefore believe, that the large NLL corrections, found in this paper, are understood and certainly do not signal the breakdown of renormalization group improved perturbation theory.

The NLL branching ratio $\mathcal{B}^{\mathrm{NLL}}(b\to sg)$ is then obtained as described in Sec. VIII. The result is shown by the solid line in Fig. 9. For the input values, we take: $m_b=(4.8\pm 0.2)$ GeV, $(m_c/m_b)=0.29\pm 0.02$, $\alpha_s(m_Z)=0.119\pm 0.003$, $|V_{ts}^* V_{tb}/V_{cb}|^2=0.95\pm 0.03$, $\mathcal{B}_{\mathrm{sl}}^{\mathrm{exp}}=(10.49\pm 0.46)\%$, and $m_t^{\mathrm{pole}}=(175\pm 5)$ GeV. As the scale depen-

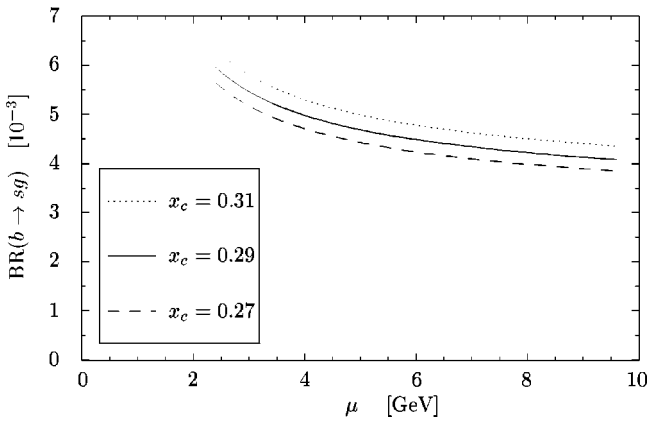

FIG. 10. NLL branching ratio $\mathcal{B}^{\rm NLL}(b\to sg)$ as a function of the scale μ for the three value of the ratio $x_c=m_c/m_b$. See text.

dence is rather large, we did not take into account the error due to the uncertainties in the input parameters. Based on Fig. 9, we obtain the NLL branching ratio

$$\mathcal{B}^{\rm NLL}(b\to sg)=(5.0\pm 1.0)\times 10^{-3}. \tag{106}$$

We would like to stress that the NLL corrections drastically enhance the LL value (see dashed line in Fig. 9) for which one obtains

$$\mathcal{B}^{\rm LL}(b\to sg)=(2.2\pm 0.8)\times 10^{-3}. \tag{107}$$

As already mentioned in the discussion of the function $\overline{D}$, the main enhancement is due to the virtual and bremsstrahlung corrections to $b\to sg$, calculated in this paper. At the level of the branching ratio, this fact is illustrated by the dotted line in Fig. 9, which is obtained by discarding $\Gamma^{\rm brems}_{\rm fin}$ and by switching off r_1, r_2, and r_8 in the expression for $\Gamma^{\rm NLL}(b\to sg)$ [see Eq. (99)].

The largest uncertainty due to the physical input parameters on $\mathcal{B}^{\rm NLL}(b\to sg)$ results from the charm quark mass. The dependence of $\mathcal{B}^{\rm NLL}(b\to sg)$ on m_c is illustrated in Fig. 10, where $x_c=m_c/m_b$ is varied between 0.27 and 0.31. Choosing $\mu=m_b$, the resulting uncertainty amounts to $\sim\pm 6\%$.

X. NUMERICAL EVALUATION OF THE CHARMLESS DECAY RATE

In this section we investigate the impact of the NLL QCD corrections to $b\to sg$ on the inclusive hadronic charmless decay rate of the $\overline{B}$ meson. At the quark level, we take into account the hadronic processes

$$b\to q'\overline{q}'q; \quad b\to sg, \tag{108}$$

where $q=d,s$ and $q'=u,d,s$. As we do not distinguish between $\Delta S=0$ and $\Delta S=1$ contributions, we can safely neglect the CKM suppressed decay mode $b\to dg$. More precisely, we calculate the CP-averaged branching ratio

$$\overline{\mathcal{B}_\ell}=\frac{\Gamma(b\to X_\ell)+\Gamma(\overline{b}\to\overline{X_\ell})}{2\Gamma_{\rm sl}}\mathcal{B}^{\rm exp}_{\rm sl}, \tag{109}$$

where X_ℓ stands for the final states listed in Eq. (108). In the numerical results for $\overline{\mathcal{B}_\ell}$ we will insert $\Gamma_{\rm sl}$ as given in Eq. (102), i.e., we do not make an α_s expansion of $1/\Gamma_{\rm sl}$ in Eq. (109). The charmless hadronic decay rate $\overline{\mathcal{B}_\ell}$ then reads

$$\overline{\mathcal{B}_\ell}=\overline{\mathcal{B}}_{sg}+\sum_{\substack{q=d,s\\ q'=u,d,s}}\overline{\mathcal{B}}_{q'\overline{q}'q}. \tag{110}$$

While the $O(\alpha_s)$ corrections to semileptonic processes have been known for a long time (see e.g., Ref. [27]), the NLL corrections to the hadronic processes in Eq. (108) with 3 quarks in the final state had a long history and were completed to a large extent only recently by Lenz *et al.* [8,6]; however, current-current type corrections to the penguin operators are still missing. To briefly summarize the history, it is useful to decompose the NLL expressions for the decay widths of these processes into various pieces. Taking as an example the process $b\to u\overline{u}d$, we write as in Ref. [8]:

$$\Gamma(b\to u\overline{u}d)=\Gamma^{(0)}+\frac{\alpha_s}{4\pi}[\Delta\Gamma_{\rm cc}+\Delta\Gamma_{\rm peng}+\Delta\Gamma_8+\Delta\Gamma_{\rm W}]. \tag{111}$$

The first two terms in the square bracket in Eq. (111) describe the effect of current-current and penguin diagrams involving the operators[5] O_1 and O_2. $\Delta\Gamma_8$ likewise contains the matrix element of the operator O_8. The remaining part $\Delta\Gamma_{\rm W}$ of the NLL contribution is made of the corrections to the Wilson coefficients multiplying the tree-level amplitudes in $\Gamma^{(0)}$. In this approximation, the matrix elements of the penguin operators $O_3,\ldots,O_6$ only enter at tree level. As the expressions for the RHS of Eq. (111) are explicitly given in Ref. [8], we do not give them here. For later reference, we denote this approximation (for lack of a better word) by ''approx1.''

Later, in Ref. [6], the same authors added the contributions of the penguin diagrams associated with the penguin operators to the decay matrix elements and took into account the interference with the tree level matrix element of the operator O_2 in the decay width. In addition, they took into account the square of the matrix element of the penguin diagram associated with O_2. Although being of next-to-NLL, this term is numerically relatively large, as it is multiplied with C_2^2. These new contributions can be absorbed into the quantity $\Delta\Gamma_{\rm new}$, which is understood to be added to the

[5]Note that the authors of Refs. [8,6] use the old operator basis [22].

TABLE II. Table for the charmless hadronic branching ratio $\overline{\mathcal{B}_\ell}$ (in %) in the various approximations discussed in the text. Unless specified explicitly in the first column, the input parameters correspond to the central values in Eq. (112).

input	approx0	approx1	approx2	with NLL $b\to sg$
as in Eq. (112)	1.32	1.50	1.62	1.88
$\mu=m_b/4$	3.86	3.21	3.34	3.62
$\mu=m_b/2$	2.06	2.09	2.18	2.43
$\mu=2m_b$	0.96	1.14	1.28	1.55
$\lvert V_{ub}/V_{cb}\rvert=0.06$	0.94	1.13	1.24	1.50
$\lvert V_{ub}/V_{cb}\rvert=0.07$	1.03	1.22	1.33	1.59
$\lvert V_{ub}/V_{cb}\rvert=0.08$	1.14	1.32	1.44	1.69
$\lvert V_{ub}/V_{cb}\rvert=0.09$	1.26	1.44	1.55	1.81
$\lvert V_{ub}/V_{cb}\rvert=0.10$	1.39	1.57	1.69	1.94
$\lvert V_{ub}/V_{cb}\rvert=0.11$	1.54	1.72	1.83	2.09
$\lvert V_{ub}/V_{cb}\rvert=0.12$	1.70	1.87	1.99	2.25
$\lvert V_{ub}/V_{cb}\rvert=0.13$	1.87	2.05	2.16	2.42
$x_c=0.25$	1.14	1.32	1.45	1.69
$x_c=0.27$	1.22	1.41	1.53	1.78
$x_c=0.29$	1.32	1.50	1.62	1.88
$x_c=0.31$	1.44	1.61	1.72	1.99
$x_c=0.33$	1.57	1.74	1.84	2.12

terms in the bracket in Eq. (111). As the extraction of $\Delta\Gamma_{\rm new}$ from Ref. [6] is straightforward, we do not give the explicit expression. This approximation, which contains—up to the current-current type corrections to the penguin operators—the full NLL contribution to the hadronic three body decays, is called ''approx2.''

We note that the approximation where only the current-current type corrections $\Delta\Gamma_{\rm cc}$ were considered together with the shifts $\Delta\Gamma_{\rm W}$ in the Wilson coefficients has existed for a long time [7]. We denote this approximation by ''approx0'' in the numerical discussion.

In Table II we present numerical results for the charmless hadronic branching ratio $\overline{\mathcal{B}_\ell}$ in the various approximations mentioned above. The process $b\to sg$, encoded in $\overline{\mathcal{B}_{sg}}$ in Eq. (110) is taken into account in the columns ''approx0,'' ''approx1'' and''approx2'' at LL precision. The last column includes in addition the NLL corrections to $b\to sg$ which were calculated in this paper. Table II was produced with the following input parameters:

$$m_b=(4.8\pm0.2)\ \text{GeV},\quad \mu=m_b,$$

$$(m_c/m_b)=0.29\pm0.04,\quad \alpha_s(m_Z)=0.119\pm0.003,$$

$$m_t^{\rm pole}=(175\pm5)\ \text{GeV},$$

$$\mathcal{B}_{\rm sl}^{\rm exp}=(10.49\pm0.46)\%$$

$$\lvert V_{us}\rvert=0.22,\quad \lvert V_{cb}\rvert=0.038,$$

$$\lvert V_{ub}/V_{cb}\rvert=0.095\pm0.035,\quad \delta=60^\circ\pm30^\circ. \tag{112}$$

The central value for $\lvert V_{ub}/V_{cb}\rvert$ corresponds to the (improved) Wolfenstein parameters $\overline{\rho}=0.20$ and $\overline{\eta}=0.37$ [28]. The remaining entries of the CKM matrix are then obtained as described in detail in [29]. We note that the averaged charmless hadronic branching ratio is practically independent of δ, as already observed in Ref. [6].

The numbers in column ''approx2'' are very similar to those in Table 1 of Ref. [6]. The small discrepancy is due to the omission of the $1/m_b^2$ power corrections in our work.

Staring from the numbers in column ''approx0,'' Table II illustrates, that the various improvements shown in the other columns are relatively large, tending to increase $\overline{\mathcal{B}_\ell}$. In particular, the NLL corrections to $b\to sg$ are of similar importance as the corrections calculated in [8,6].

For $\lvert V_{ub}/V_{cb}\rvert=0.095$ we obtain the charmless hadronic branching ratio

$$\overline{\mathcal{B}_\ell}=(1.88^{+0.60}_{-0.38})\%, \tag{113}$$

where the error corresponds to a variation of $x_c=(m_c/m_b)$ and of the renormalization scale μ in the ranges $0.25\leqslant x_c\leqslant 0.33$ and $0.5\leqslant\mu/m_b\leqslant 2.0$. The corresponding errors are added in quadrature. The experimental uncertainty in $\alpha_s(m_Z)$ has a smaller impact and the errors due to the remaining input parameters in Eq. (112) are negligible. The large renormalization scale dependence of this result is expected to be weakened once the current-current type corrections to the penguin operators are included.

So far, we have considered the *charmless hadronic* branching ratio $\overline{\mathcal{B}_\ell}$. To obtain the *total charmless* branching ratio $\overline{\mathcal{B}}(B\to\text{no charm})$, one has to add twice the charmless semileptonic branching ratio $\mathcal{B}(B\to X_u l\overline{\nu}_l)$, for $l=e$ and $l=\mu$ [27] (the contribution for $l=\tau$, as well as radiative decay modes can be safely neglected):

$$\mathcal{B}(B\to X_u l\overline{\nu}_l)=(0.17\pm0.03)\%\times\left(\frac{\lvert V_{ub}/V_{cb}\rvert}{0.095}\right)^2. \tag{114}$$

For $\lvert V_{ub}/V_{cb}\rvert=0.095$, we find

$$\overline{\mathcal{B}}(B\to\text{no charm})=(2.22^{+0.60}_{-0.38})\%. \tag{115}$$

The experimental result for the total charmless branching ratio reads

$$\overline{\mathcal{B}}^{\rm exp}(B\to\text{no charm})=(0.2\pm4.1)\%, \tag{116}$$

obtained in Ref. [30] from CLEO data [31].

XI. NUMERICAL PREDICTIONS IN THE PRESENCE OF ENHANCED $C_8^{\rm eff}$

As discussed in the Introduction, the theoretical prediction of the semileptonic branching ratio and the charm multiplicity are compatible with the experimental findings if the renormalization scale is allowed to be as low as $m_b/4$. Both predictions are, however, at the lower side and therefore an enhancement of the charmless hadronic branching ratio $\overline{\mathcal{B}_\ell}$

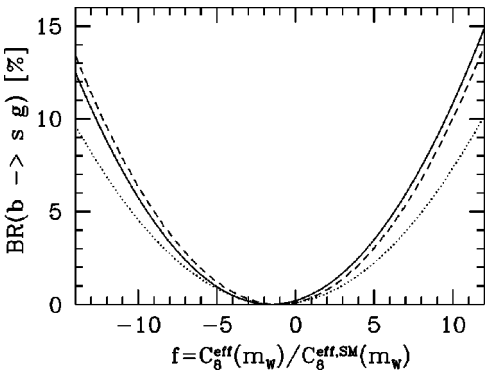

FIG. 11. Branching ratio $\mathcal{B}(b\to sg)$ as a function of $f=C_8^{\rm eff}(m_W)/C_8^{\rm eff,SM}(m_W)$. For the exact definition of f, see Eq. (117). The dotted (solid) curve shows the LL (NLL) approximation. The dashed curve is obtained by switching off the matrix elements of the operators O_1 and O_2.

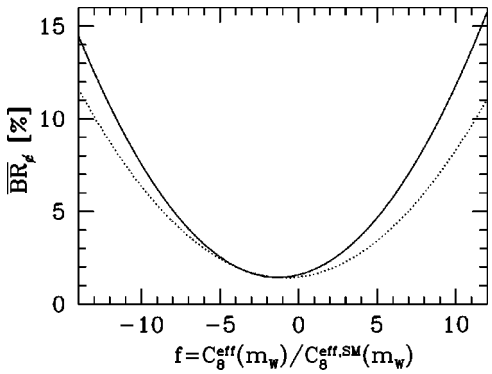

FIG. 12. Charmless hadronic branching ratio $\overline{\mathcal{B}_\ell}$ as a function of $f=C_8^{\rm eff}(m_W)/C_8^{\rm eff,SM}(m_W)$. For the exact definition of f, see Eq. (117). The dotted (solid) curve includes the LL (NLL) approximation for $\mathcal{B}(b\to sg)$. The NLL corrections to the decay modes with three quark in the final state (see ''approx2'' in Sec. X) are included in both cases.

by new physics would lead to a better agreement. It is therefore still conceivable that $\overline{\mathcal{B}_\ell}$ is considerably larger than in the standard model (SM).

In the SM the initial conditions for C_{3-6} and C_8 are generated at a scale $\mu=O(m_W)$ by the one-loop bsg vertex function. Because of the fact that the W-boson only couples to left-handed quarks, only chromomagnetic operators proportional to m_b (and m_s) are generated. In extensions of the SM, however, also chromomagnetic operators where m_b (or m_s) is replaced by the mass of a heavy particle propagating in the loop, can be generated [32]. Such operators potentially lead to large contributions to $b\to sg$. In the following we will perform a model independent analysis of the impact of enhanced C_8 on $\overline{\mathcal{B}_\ell}$, emphasizing the role of the NLL corrections to $b\to sg$. We assume that only chromomagnetic operators with the same helicity structure as O_8 in the SM are generated which can then be described as a shift in C_8. For simplicity, we further assume that the CKM structure of the new contribution is the same as in the SM, hence neglecting the possibility of new CP-violating phases, by assuming the shift in C_8 to be real.

In Fig. 11 we investigate the impact of enhanced $C_8^{\rm eff}(m_W)=C_8^{0,\rm eff}(m_W)+\alpha_s/(4\pi)C_8^{1,\rm eff}(m_W)$ on the branching ratio for $b\to sg$. In the NLL approximation for this branching ratio, both, $C_8^{0,\rm eff}(m_W)$ and $C_8^{1,\rm eff}(m_W)$ enter. In general, it is expected that the two pieces get different new physics shifts. For purpose of illustration, we assume however that both pieces are the same multiple f of the SM counterparts; i.e., we assume that

$$C_8^{0,\rm eff}(m_W)=fC_8^{0,\rm eff,SM}(m_W);\quad C_8^{1,\rm eff}(m_W)=fC_8^{1,\rm eff,SM}(m_W). \tag{117}$$

The dotted curve shows the LL prediction of $\mathcal{B}(b\to sg)$ as a function of f, while the solid curve shows the NLL prediction. It is expected that for large enhancement factors, the matrix elements of the operators O_1 and O_2 become unimportant; this feature is illustrated by the dashed line, which is obtained by switching off these matrix elements. The NLL corrections (for large enhancement factors) amount to almost 50% of the LL prediction.

In Fig. 12, the impact of enhanced C_8 on the charmless hadronic branching ratio $\overline{\mathcal{B}_\ell}$ is illustrated. The dotted curve includes the NLL corrections to the decay modes with three quark in the final state and the LL result for $\mathcal{B}(b\to sg)$ (see ''approx2'' in Sec. X), while the solid curve also includes the NLL corrections to $\mathcal{B}(b\to sg)$. For a given value of $\overline{\mathcal{B}_\ell}$ (from an ideal measurement), $C_8(m_W)$ can be measured in principle. To illustrate this, we take the hypothetical value $\overline{\mathcal{B}_\ell}=5\%$. The two solutions for the enhancement factor f are $f=7$ and $f=-9$ when using the dotted curve; including NLL corrections to $b\to sg$ (solid curve), enhancement factors with smaller absolute values do the job, viz. $f=5$ and $f=-8$.

XII. SUMMARY

In this paper we presented a detailed calculation of the $O(\alpha_s)$ virtual corrections to the decay width $\Gamma(b\to sg)$. The most difficult part, the two-loop diagrams associated with the operators O_1 and O_2 which from the numerical point of view play a crucial role, was obtained by using Mellin-Barnes techniques. Also complete expressions for the corresponding $O(\alpha_s)$ bremsstrahlung corrections to $b\to sg$ were given. The combined result is free of infrared and collinear singularities, in accordance with the Kinoshita-Lee-Nauenberg (KLN) theorem.

The renormalized virtually corrected matrix element $\langle sg|O_8|b\rangle$ contains logarithms of the form $\ln(m_f/\mu)(f=u,d,s,c,b)$, which for the light flavors (u,d,s) represent a special kind of singularity. Keeping in mind that these terms originate from the renormalization factor Z_3 of the gluon field. i.e., from gluon self energy diagrams in which these flavors propagate, we argued that these singularities cancel against the logarithms present in the decay rate $\Gamma(b\to sf\bar{f})$ with $f=u,d,s$. We therefore included the O_8 contribution to

$\Gamma(b\to sf\bar{f})$ for $f=u,d,s$; we also mentioned other possibilities to deal with these terms.

Taking into account the existing next-to-leading logarithmic (NLL) result for the Wilson coefficient $C_8^{\rm eff}$, a complete NLL result for the branching ratio $\mathcal{B}^{\rm NLL}(b\to sg)$ was obtained. Numerically, we found $\mathcal{B}^{\rm NLL}=(5.0\pm 1.0)\times 10^{-3}$, which is more than a factor of two larger than the leading logarithmic result $\mathcal{B}^{\rm LL}=(2.2\pm 0.8)\times 10^{-3}$.

We then investigated the impact of these corrections on the inclusive charmless hadronic branching ratio $\overline{\mathcal{B}_\ell}$ of B mesons. We found that the NLL corrections calculated in this paper are of similar importance as NLL corrections to b-quark decay modes with three quarks in the final state, which were presented by Lenz *et al.* [8,6].

Finally, the impact of the NLL corrections to $b\to sg$ on $\overline{\mathcal{B}_\ell}$ was studied in scenarios, where the Wilson coefficient C_8 is enhanced by new physics. For a given value of $\overline{\mathcal{B}_\ell}$ (from an ideal measurement), $C_8(m_W)$ can be measured in principle. To illustrate this, we took the hypothetical value $\overline{\mathcal{B}_\ell}=5\%$. The two solutions for the enhancement factor f are $f=7$ and $f=-9$, using the LL approximation for $\mathcal{B}(b\to sg)$; including NLL corrections to $b\to sg$, somewhat smaller enhancement factors ($f=5$ and $f=-8$) are needed to obtain the hypothetical value $\overline{\mathcal{B}_\ell}=5\%$.

ACKNOWLEDGMENTS

We would like to thank A. Ali, A. Kagan, A. Lenz, P. Minkowski, M. Neubert, and U. Nierste for helpful discussions. This work was partially supported by Schweizerischer Nationalfonds.

APPENDIX A: NEXT-TO-LEADING ORDER WILSON COEFFICIENTS

In this appendix we present the explicit formulas which allow to calculate the Wilson coefficients needed in this paper.

In Sec. A 1, we give the results for the Wilson coefficients at the matching scale μ_W, which is usually taken to be of order m_W. Section A 2 is devoted to the the Wilson coefficients at the scale μ_b, where μ_b is of order m_b. We give an explicit expression for $C_8^{\rm eff}(\mu_b)$ at NLL, which is new. To make this appendix self-contained, we also repeat the results for the Wilson coefficients $C_1(\mu_b)$ and $C_2(\mu_b)$ which are needed only to LL precision in our application.

1. NLL Wilson coefficients at the matching scale μ_W

To give the results for the effective Wilson coefficients $C_i^{\rm eff}$ at the matching scale μ_W in a compact form, we write[6]

$$C_i^{\rm eff}(\mu_W)=C_i^{0,\rm eff}(\mu_W)+\frac{\alpha_s(\mu_W)}{4\pi}C_i^{1,\rm eff}(\mu_W). \qquad \text{(A1)}$$

[6]Note that $C_i^{\rm eff}(\mu)=C_i(\mu)$ by definition for $i=1,\ldots,6$.

The LL Wilson coefficients at this scale are well known [33,34]:

$$\begin{aligned}
&C_2^{0,\rm eff}(\mu_W)=1\\
&C_i^{0,\rm eff}(\mu_W)=0 \quad (i=1,3,4,5,6)\\
&C_7^{0,\rm eff}(\mu_W)=\frac{x}{24}\left[\frac{-8x^3+3x^2+12x-7+(18x^2-12x)\ln x}{(x-1)^4}\right]\\
&C_8^{0,\rm eff}(\mu_W)=\frac{x}{8}\left[\frac{-x^3+6x^2-3x-2-6x\ln x}{(x-1)^4}\right].
\end{aligned} \qquad \text{(A2)}$$

The coefficients $C_7^{0,\rm eff}(\mu_W)$ and $C_8^{0,\rm eff}(\mu_W)$ are functions of $x=m_t^2/m_W^2$. Note that there is no *explicit* dependence of the matching scale μ_W in these functions. Whether there is an *implicit* μ_W dependence via the t-quark mass depends on the precise definition of this mass which has to be specified when going beyond leading logarithms. If one chooses to work with $\overline{m}_t(\mu_W)$, then there is such an implicit μ_W dependence of the lowest order Wilson coefficient; in contrast, when working with the pole mass m_t there is no such dependence. We choose to express our NLL results in terms of the pole mass m_t.

The NLL pieces $C_i^{1,\rm eff}(\mu_W)$ of the Wilson coefficients have an explicit dependence on the matching scale μ_W and for $i=7,8$ they also explicitly depend on the actual definition of the t-quark mass. Initially, when the heavy particles are integrated out, it is convenient to work out the matching conditions $C_i^{1,\rm eff}(\mu_W)$ for $i=7,8$ in terms of $\overline{m}_t(\mu_W)$. Using Eq. (5), it is then straightforward to get the corresponding result expressed in terms of the pole mass m_t. One obtains for $i=1,\ldots,6$:

$$\begin{aligned}
&C_1^{1,\rm eff}(\mu_W)=15+6\ln\frac{\mu_W^2}{m_W^2},\\
&C_4^{1,\rm eff}(\mu_W)=E_0+\frac{2}{3}\ln\frac{\mu_W^2}{m_W^2},\\
&C_i^{1,\rm eff}(\mu_W)=0 \quad (i=2,3,5,6)
\end{aligned} \qquad \text{(A3)}$$

with

$$\begin{aligned}
E_0=&\frac{x(x^2+11x-18)}{12(x-1)^3}+\frac{x^2(4x^2-16x+15)}{6(x-1)^4}\ln x\\
&-\frac{2}{3}\ln x-\frac{2}{3}.
\end{aligned} \qquad \text{(A4)}$$

For $i=7,8$, we split $C_i^{1,\rm eff}(\mu_W)$ into three terms:

$$C_i^{1,\rm eff}(\mu_W)=W_i+M_i\ln\frac{\mu_W^2}{m_W^2}+T_i\left(\ln\frac{m_t^2}{\mu_W^2}-\frac{4}{3}\right). \qquad \text{(A5)}$$

The first two terms W_i and M_i would be the full result when working in terms of $\overline{m}_t(\mu_W)$. T_i results when expressing $\overline{m}_t(\mu_W)$ in terms of the pole mass m_t in the corresponding lowest order coefficients. Thus, for $i=7,8$, the term T_i is obtained as

$$T_i = 8x \frac{\partial C_i^{0,\,\mathrm{eff}}(\mu_W)}{\partial x}. \tag{A6}$$

The explicit form of the functions W_i, M_i, and T_i reads

$$W_7 = \frac{-16x^4-122x^3+80x^2-8x}{9(x-1)^4}\mathrm{Li}_2\left(1-\frac{1}{x}\right)+\frac{6x^4+46x^3-28x^2}{3(x-1)^5}\ln^2 x$$
$$+\frac{-102x^5-588x^4-2262x^3+3244x^2-1364x+208}{81(x-1)^5}\ln x+\frac{1646x^4+12205x^3-10740x^2+2509x-436}{486(x-1)^4}$$

$$W_8 = \frac{-4x^4+40x^3+41x^2+x}{6(x-1)^4}\mathrm{Li}_2\left(1-\frac{1}{x}\right)+\frac{-17x^3-31x^2}{2(x-1)^5}\ln^2 x$$
$$+\frac{-210x^5+1086x^4+4893x^3+2857x^2-1994x+280}{216(x-1)^5}\ln x+\frac{737x^4-14102x^3-28209x^2+610x-508}{1296(x-1)^4}$$

$$M_7 = \frac{82x^5+301x^4+703x^3-2197x^2+1319x-208-(162x^4+1242x^3-756x^2)\ln x}{81(x-1)^5}$$

$$M_8 = \frac{77x^5-475x^4-1111x^3+607x^2+1042x-140+(918x^3+1674x^2)\ln x}{108(x-1)^5}$$

$$T_7 = \frac{x}{3}\left[\frac{47x^3-63x^2+9x+7-(18x^3+30x^2-24x)\ln x}{(x-1)^5}\right]$$

$$T_8 = 2x\left[\frac{-x^3-9x^2+9x+1+(6x^2+6x)\ln x}{(x-1)^5}\right]. \tag{A7}$$

The dilogarithm $\mathrm{Li}_2(x)$ is defined by

$$\mathrm{Li}_2(x) = -\int_0^x \frac{dt}{t}\ln(1-t). \tag{A8}$$

2. NLL Wilson coefficients at the low scale μ_b

The evolution from the matching scale μ_W down to the low-energy scale μ_b is described by the renormalization group equation

$$\mu\frac{d}{d\mu}C_i^{\mathrm{eff}}(\mu) = C_j^{\mathrm{eff}}(\mu)\,\gamma_{ji}^{\mathrm{eff}}(\mu). \tag{A9}$$

The initial conditions $C_i^{\mathrm{eff}}(\mu_W)$ for this equation are given in Sec. A 1, while the anomalous dimension matrix $\gamma_{ij}^{\mathrm{eff}}$ up to order α_s^2 can be found in Ref. [19]. For completeness we display the result here. The anomalous dimension matrix can be expanded perturbatively as

$$\gamma_{ji}^{\mathrm{eff}}(\mu) = \frac{\alpha_s(\mu)}{4\pi}\gamma_{ji}^{0,\mathrm{eff}} + \frac{\alpha_s^2(\mu)}{(4\pi)^2}\gamma_{ji}^{1,\mathrm{eff}} + \mathcal{O}(\alpha_s^3) \tag{A10}$$

where matrix $\gamma_{ji}^{0,\mathrm{eff}}$ is given by

$$\{\gamma_{ji}^{0,\mathrm{eff}}\}=\begin{pmatrix} -4 & \frac{8}{3} & 0 & -\frac{2}{9} & 0 & 0 & -\frac{208}{243} & \frac{173}{162} \\ 12 & 0 & 0 & \frac{4}{3} & 0 & 0 & \frac{416}{81} & \frac{70}{27} \\ 0 & 0 & 0 & -\frac{52}{3} & 0 & 2 & -\frac{176}{81} & \frac{14}{27} \\ 0 & 0 & -\frac{40}{9} & -\frac{100}{9} & \frac{4}{9} & \frac{5}{6} & -\frac{152}{243} & -\frac{587}{162} \\ 0 & 0 & 0 & -\frac{256}{3} & 0 & 20 & -\frac{6272}{81} & \frac{6596}{27} \\ 0 & 0 & -\frac{256}{9} & \frac{56}{9} & \frac{40}{9} & -\frac{2}{3} & \frac{4624}{243} & \frac{4772}{81} \\ 0 & 0 & 0 & 0 & 0 & 0 & \frac{32}{3} & 0 \\ 0 & 0 & 0 & 0 & 0 & 0 & -\frac{32}{9} & \frac{28}{3} \end{pmatrix}, \tag{A11}$$

and in the $\overline{\mathrm{MS}}$ scheme with fully anticommuting γ_5, $\gamma_{ji}^{1,\mathrm{eff}}$ is

$$\{\gamma_{ji}^{1,\mathrm{eff}}\}=\begin{pmatrix} -\frac{355}{9} & -\frac{502}{27} & -\frac{1412}{243} & -\frac{1369}{243} & \frac{134}{243} & -\frac{35}{162} & -\frac{818}{243} & \frac{3779}{324} \\ -\frac{35}{3} & -\frac{28}{3} & -\frac{416}{81} & \frac{1280}{81} & \frac{56}{81} & \frac{35}{27} & \frac{508}{81} & \frac{1841}{108} \\ 0 & 0 & -\frac{4468}{81} & -\frac{31\,469}{81} & \frac{400}{81} & \frac{3373}{108} & \frac{22\,348}{243} & \frac{10\,178}{81} \\ 0 & 0 & -\frac{8158}{243} & -\frac{59\,399}{243} & \frac{269}{486} & \frac{12\,899}{648} & -\frac{17\,584}{243} & -\frac{17\,247\,1}{648} \\ 0 & 0 & -\frac{25\,168\,0}{81} & -\frac{12\,864\,8}{81} & \frac{23\,836}{81} & \frac{6106}{27} & \frac{11\,836\,96}{729} & \frac{29\,012\,96}{243} \\ 0 & 0 & \frac{58\,640}{243} & -\frac{26\,348}{243} & -\frac{14\,324}{243} & -\frac{2551}{162} & \frac{24\,803\,44}{2187} & -\frac{32\,962\,57}{729} \\ 0 & 0 & 0 & 0 & 0 & 0 & \frac{4688}{27} & 0 \\ 0 & 0 & 0 & 0 & 0 & 0 & -\frac{2192}{81} & \frac{4063}{27} \end{pmatrix}. \tag{A12}$$

The solution of Eq. (A9), obtained through the procedure described in [29], yields for the coefficient $C_8^{\mathrm{eff}}(\mu_b)$, which we decompose as

$$C_8^{\mathrm{eff}}(\mu_b)=C_8^{0,\mathrm{eff}}(\mu_b)+\frac{\alpha_s(\mu_b)}{4\pi}C_8^{1,\mathrm{eff}}(\mu_b), \tag{A13}$$

the LL term

$$C_8^{0,\mathrm{eff}}(\mu_b)=\eta^{14/23}C_8^{0,\mathrm{eff}}(\mu_W)+\sum_{i=1}^{5}h_i'\,\eta^{a_i'}C_2^{0,\mathrm{eff}}(\mu_W), \tag{A14}$$

and the NLL contribution

$$C_8^{1,\mathrm{eff}}(\mu_b)=\eta^{37/23}C_8^{1,\mathrm{eff}}(\mu_W)+6.7441(\eta^{37/23}-\eta^{14/23})C_8^{0,\mathrm{eff}}(\mu_W)$$
$$+\sum_{i=1}^{8}(e_i'\,\eta C_4^{1,\mathrm{eff}}(\mu_W)+(f_i'+k_i'\,\eta)C_2^{0,\mathrm{eff}}(\mu_W)+l_i'\,\eta C_1^{1,\mathrm{eff}}(\mu_W))\eta^{a_i}. \tag{A15}$$

The symbol η is defined as $\eta=\alpha_s(\mu_W)/\alpha_s(\mu_b)$; the vectors a_i, a_i', h_i', e_i', f_i', k_i', and l_i' read

$$\{a_i\}=\{\tfrac{14}{23},\tfrac{16}{23},\tfrac{6}{23},-\tfrac{12}{23},0.4086,-0.4230,-0.8994,0.1456\}$$
$$\{a_i'\}=\{\tfrac{14}{23},0.4086,-0.4230,-0.8994,0.1456\}$$
$$\{h_i'\}=\{\tfrac{313063}{363036},-0.9135,0.0873,-0.0571,0.0209\}$$
$$\{e_i'\}=\{2.1399,0,0,0,-2.6788,0.2318,0.3741,-0.0670\}$$
$$\{f_i'\}=\{-5.8157,0,1.4062,-3.9895,3.2850,3.6851,-0.1424,0.6492\}$$
$$\{k_i'\}=\{3.7264,0,0,0,-3.2247,0.3359,0.3812,-0.2968\}$$
$$\{l_i'\}=\{0.2169,0,0,0,-0.1793,-0.0730,0.0240,0.0113\}. \tag{A16}$$

As already mentioned earlier, we neglect the contributions of the operators $O_3,\ldots,O_6$ in our analysis for $b\to sg$, as their Wilson coefficients are rather small. We therefore only list the results for the coefficients $C_1^{\mathrm{eff}}(\mu_b)$ and $C_2^{\mathrm{eff}}(\mu_b)$, which are needed to LL precision only:

$$C_1^{0,\mathrm{eff}}(\mu_b)=(\eta^{6/23}-\eta^{-12/23})C_2^{0,\mathrm{eff}}(\mu_W)$$
$$C_2^{0,\mathrm{eff}}(\mu_b)=\left(\frac{2}{3}\eta^{6/23}+\frac{1}{3}\eta^{-12/23}\right)C_2^{0,\mathrm{eff}}(\mu_W). \tag{A17}$$

When calculating NLL results in the numerical analysis, we use the NLL expression for the strong coupling constant:

$$\alpha_s(\mu)=\frac{\alpha_s(m_Z)}{v(\mu)}\left[1-\frac{\beta_1}{\beta_0}\frac{\alpha_s(m_Z)}{4\pi}\frac{\ln v(\mu)}{v(\mu)}\right], \tag{A18}$$

with

$$v(\mu)=1-\beta_0\frac{\alpha_s(m_Z)}{2\pi}\ln\left(\frac{m_Z}{\mu}\right), \tag{A19}$$

where $\beta_0=\frac{23}{3}$ and $\beta_1=\frac{116}{3}$ (for 5 flavors). However, for LL results we always use the LL expression for $\alpha_s(\mu)$, i.e., β_1 is put to zero in Eq. (A18).

APPENDIX B: ONE-LOOP FUNCTIONS $G_{-1}(t)$ AND $G_0(t)$

In this appendix we give the explicit results for the functions $G_{-1}(t)$ and $G_0(t)$ needed in Eq. (83). Evaluating the integral in Eq. (78) for $i=-1,0$, one obtains

$$G_{-1}(t)=\begin{cases}-\dfrac{\pi^2}{2}+2\ln^2\left(\dfrac{\sqrt{t}+\sqrt{t-4}}{2}\right)-2i\pi\ln\left(\dfrac{\sqrt{t}+\sqrt{t-4}}{2}\right); & t\geqslant 4\\ -\dfrac{\pi^2}{2}-2\arctan^2\left(\sqrt{\dfrac{4-t}{t}}\right)+2\pi\arctan\left(\sqrt{\dfrac{4-t}{t}}\right); & 0\leqslant t\leqslant 4\end{cases} \tag{B1}$$

$$G_0(t)=\begin{cases}-2+2\sqrt{\dfrac{t-4}{t}}\ln\left(\dfrac{\sqrt{t}+\sqrt{t-4}}{2}\right)-i\pi\sqrt{\dfrac{t-4}{t}}; & t\geqslant 4\\ -2-2\sqrt{\dfrac{4-t}{t}}\arctan\left(\sqrt{\dfrac{4-t}{t}}\right)+\pi\sqrt{\dfrac{4-t}{t}}; & 0\leqslant t\leqslant 4.\end{cases} \tag{B2}$$

[1] I. Bigi *et al.*, Phys. Rev. Lett. **71**, 496 (1993); A. Manohar and M. B. Wise, Phys. Rev. D **49**, 1310 (1994); B. Blok *et al.*, *ibid.* **49**, 3356 (1994); T. Mannel, Nucl. Phys. **B413**, 396 (1994); A. Falk, M. Luke, and M. Savage, Phys. Rev. D **49**, 3367 (1994).
[2] I. Bigi *et al.*, Phys. Lett. B **293**, 430 (1992); **297**, 477(E) (1993).
[3] I. Bigi *et al.*, in *B decays*, 2nd ed. edited by S. Stone (World Scientific, Singapore, 1994), p. 132; I. Bigi, hep-ph/9508408.
[4] M. Neubert and C. T. Sachrajda, Nucl. Phys. **B483**, 339 (1997).
[5] I. J. Kroll, *Proceedings of the 17th International Symposium on Lepton Photon Interactions*, Beijing, P. R. China, 1995, p. 204, hep-ex/9602005.
[6] A. Lenz, U. Nierste, and G. Ostermaier, Phys. Rev. D **59**, 034008 (1999).
[7] G. Altarelli and S. Petrarca, Phys. Lett. B **261**, 303 (1991).
[8] A. Lenz, U. Nierste, and G. Ostermaier, Phys. Rev. D **56**, 7228 (1997).
[9] C. Greub and P. Liniger, Phys. Lett. B **494**, 237 (2000).
[10] I. Bigi *et al.*, Phys. Lett. B **323**, 408 (1994); A. Falk, M. B. Wise, and I. Dunietz, Phys. Rev. D **51**, 1183 (1995); I. Dunietz *et al.*, Eur. Phys. J. C **1**, 211 (1998); H. Yamamoto, hep-ph/9912308.
[11] E. Bagan *et al.*, Nucl. Phys. **B432**, 3 (1994); Phys. Lett. B **342**, 362 (1995); **374**, 363(E) (1996); E. Bagan *et al.*, *ibid.* **351**, 546 (1995).
[12] A. Golutvin, plenary talk given at the XXXth International Conference on High Energy Physics, Osaka, Japan, 2000.
[13] A. L. Kagan and J. Rathsman, hep-ph/9701300.
[14] M. Douadi, in Proceedings of the International Conference on High Energy Physics, Jerusalem, Israel, 1997.
[15] A. L. Kagan, in Proceedings of the 2nd International Conference on B Physics and CP Violation, Honolulu, Hawaii, USA, 1997, hep-ph/9806266.
[16] M. Ciuchini *et al.*, Phys. Lett. B **334**, 137 (1994).
[17] W. S. Hou, A. Soni, and H. Steger, Phys. Rev. Lett. **59**, 1521 (1987); W. S. Hou, Nucl. Phys. **B308**, 561 (1988).
[18] H. Simma and D. Wyler, Nucl. Phys. **B344**, 283 (1990).
[19] K. Chetyrkin, M. Misiak, and M. Münz, Phys. Lett. B **400**, 206 (1997); Nucl. Phys. **B518**, 473 (1998); **B520**, 279 (1998).
[20] K. Adel and Y. P. Yao, Phys. Rev. D **49**, 4945 (1994); C. Greub and T. Hurth, *ibid.* **56**, 2934 (1997); M. Ciuchini *et al.*, Nucl. Phys. **B527**, 21 (1998); A. J. Buras, A. Kwiatkowski, and N. Pott, *ibid.* **B517**, 353 (1998).
[21] A. J. Buras, M. Jamin, M. E. Lautenbacher, and P. H. Weisz, Nucl. Phys. **B370**, 69 (1992); **B375**, 501 (1992); M. Ciuchini, E. Franco, G. Martinelli, L. Reina, and L. Silvestrini, Phys. Lett. B **316**, 127 (1993); M. Ciuchini, E. Franco, L. Reina, and L. Silvestrini, Nucl. Phys. **B421**, 41 (1994); M. Ciuchini, E. Franco, G. Martinelli, and L. Reina, Phys. Lett. B **301**, 263 (1993); Nucl. Phys. **B415**, 403 (1994); M. Ciuchini, E. Franco, G. Martinelli, L. Reina, and L. Silvestrini, Phys. Lett. B **334**, 137 (1994); M. Misiak, Nucl. Phys. **B393**, 23 (1993); **B439**, 461(E) (1995); G. Cella, G. Curci, G. Ricciardi, and A. Viceré, Phys. Lett. B **325**, 227 (1994); Nucl. Phys. **B431**, 417 (1994); A. J. Buras, M. Misiak, M. Münz, and S. Pokorski, *ibid.* **B424**, 374 (1994); M. Misiak and M. Münz, Phys. Lett. B **344**, 308 (1995).
[22] B. Grinstein, R. Springer, and M. B. Wise, Phys. Lett. B **202**, 138 (1988); Nucl. Phys. **B339**, 269 (1990).
[23] *Pocketbook of Mathematical Functions*, edited by M. Abramowitz and I. Stegun (Verlag Harri Deutsch, Frankfurt/Main, 1984).
[24] C. Greub, T. Hurth, and D. Wyler, Phys. Lett. B **380**, 385 (1996); Phys. Rev. D **54**, 3350 (1996).
[25] V. A. Smirnov, *Renormalization and Asymptotic Expansions* (Birkhäuser, Basel, 1991); E. E. Boos and A. I. Davydychev, Theor. Math. Phys. **89**, 1052 (1992); N. I. Usyukina, Theor. Math. Phys. **79**, 385 (1989); **22**, 211 (1975); *Higher Transcendental Functions*, edited by A. Erdelyi (McGraw Hill, New York, 1953).
[26] A. Ali and C. Greub, Z. Phys. C **49**, 431 (1991); **60**, 433 (1993); Phys. Lett. B **259**, 182 (1991); **361**, 146 (1995); N. Pott, Phys. Rev. D **54**, 938 (1996).
[27] Y. Nir, Phys. Lett. B **221**, 184 (1989).
[28] A. Ali and D. London, Eur. Phys. J. C **9**, 687 (1999); hep-ph/0002167.
[29] G. Buchalla, A. Buras, and M. Lautenbacher, Rev. Mod. Phys. **68**, 1125 (1996).
[30] M. Neubert, in Proceedings of the International Conference on High Energy Physics, Jerusalem, Israel, 1997, hep-ph/9801269.
[31] CLEO Collaboration, T. E. Coan *et al.*, Phys. Rev. Lett. **80**, 1150 (1998).
[32] S. Bertolini, F. Borzumati, and A. Masiero, Nucl. Phys. **B294**, 321 (1987); A. L. Kagan, Phys. Rev. D **51**, 6196 (1995); M. Ciuchini, E. Gabrielli, and G. F. Giudice, Phys. Lett. B **388**, 353 (1996); A. L. Kagan and J. Rathsman, hep-ph/9701300; F. Borzumati, C. Greub, T. Hurth, and D. Wyler, Phys. Rev. D **62**, 075005 (2000).
[33] T. Inami and C. S. Lim, Prog. Theor. Phys. **65**, 297 (1981).
[34] W. S. Hou and R. S. Willey, Phys. Lett. B **202**, 591 (1988).